KADIR HAS UNIVERSITY
GRADUATE SCHOOL OF SCIENCE AND ENGINEERING

ANALYSIS OF VISIBLE LIGHT COMMUNICATION SYSTEMS AND ADAPTIVE EQUALIZATION EFFECTS

MASTER THESIS

ATİLLA MAMUŞ

November, 2015

ANALYSIS OF VISIBLE LIGHT COMMUNICATION SYSTEMS AND ADAPTIVE EQUALIZATION EFFECTS

ATİLLA MAMUŞ

Submitted to the Graduate School of Science and Engineering
in partial fulfillment of the requirements for the degree of
Master of Science
in
ELECTRONICS ENGINEERING

KADIR HAS UNIVERSITY
November, 2015

KADIR HAS UNIVERSITY

GRADUATE SCHOOL OF SCIENCE AND ENGINEERING

ANALYSIS OF VISIBLE LIGHT COMMUNICATION SYSTEMS AND ADAPTIVE EQUALIZATION EFFECTS

ATİLLA MAMUŞ

APPROVED BY:

Prof. Dr. Erdal Panayırcı (Advisor) (KHU) _____

Assoc. Prof. Dr. Serhat Erküçük (KHU) _____

Assoc. Prof. Dr. Hakan Doğan (IU) _____

APPROVAL DATE: 24/11/2015

"I, Atilla Mamuş, confirm that the work presented in this thesis is my own. Where information has been derived from other sources, I confirm that this has been indicated in the thesis."

_____

ATİLLA MAMUŞ

ABSTRACT

ANALYSIS OF VISIBLE LIGHT COMMUNICATION SYSTEMS AND ADAPTIVE EQUALIZATION EFFECTS

Atilla Mamuş

Master of Science in Electronics Engineering

Advisor: Prof. Dr. Erdal Panayırcı

November, 2015

Communication by means of visible light is a newly developing technology that has been brought up as an alternative to the current electromagnetic based communication systems. The recently conducted studies led to the use of LED Technology for illumination purposes and for this technology to have an edge over devices that consume excessive energy as presently being used by us. LED technology is predicted to become an important part of illumination systems especially in consideration of the low energy consumption, low voltage use, product longevity and small size the technology can provide. Furthermore, the use of semi-conductor materials in the LED technology lends this illumination tool the capability to be turned on and off very fast in comparison to the other similar purpose devices. This capability makes it possible for LED technology to be used as a means of data transmission in addition to being a means of illumination. Studies are being conducted to use LEDs effectively as an optic transmission transmitter antenna and application of modulation techniques used in electromagnetic systems to VLC technology for purposes of achieving resistance against white noise, reflections, refractions and echoes. In literature, the model of receiving data by means of adaptive filters and its processing has been used in very limited number of studies and in these studies, generally LMS algorithms were used. In this dissertation, an empty room in rectangular prism shape in pre-determined dimensions was used with LED panels, in numbers and positions previously determined, which sent data, whereby, the impulse response displayed by the channel until the data sent that reached the photo detector was analyzed according to different FOV angles in

computer environment and later on, the data was sent to the receiver through these channels that have differing impulse response based on specific FOV degrees. The data that is processed at the receiver was passed through adaptive filters to evaluate byte error rate performances in the computer environment. LMS and RLS algorithms were used in the adaptive filter. The simulation results have been displayed in graphics of bit error rate change based on SNR, and it has been observed that the adaptive filter on which RLS algorithm is used provided better results than the adaptive filter on which LMS algorithm was used.

Keywords: Visible Light Communication, Equalization, LMS, RLS

ÖZET

GÖRÜNÜR IŞIKLA İLETİŞİM SİSTEMİNİN VE ADAPTİF KANAL DENKLEŞTİRİCİ ETKİSİNİN ANALİZİ

Atilla Mamuş

Elektronik Mühendisliği, Yüksek Lisans

Danışman: Prof. Dr. Erdal Panayırcı

Kasım, 2015

Görünür ışıkla iletişim yeni gelişmekte olan bir teknoloji olup bugünkü elektromanyetik kökenli iletişim sistemlerine karşı alternatif bir sistem olarak gösterilmektedir. Yakın zamana kadar yapılan çalışmalar LED teknolojisinin aydınlatma aracı olarak kullanılmasına ve günümüzde kullanılan aşırı enerji tüketen cihazlara karşı üstünlük sağlamasına sebep olmuştur. Düşük güç tüketimi, düşük voltaj kullanımı, uzun ömürlü olması, ve küçük boyutlu olmaları sebebiyle LED'ler geleceğin aydınlatma sistemlerinin en önemli parçalarından biri olacağı öngörülmektedir. Ayrıca LED teknolojisinin temelinde yarı iletken materyallerin kullanılması bu aydınlatma aracına, diğer aydınlatma araçlarına uygulanamayacak derecede çok hızlı açılıp kapanma özelliğini de vermektedir. İşte bu özellik LED teknolojisini bir aydınlatma aracı olarak kullanılmasının dışında bir veri iletim aracı olarak kullanılmasına da imkan sağlamaktadır. LED'lerin bir optik iletim verici anteni olarak etkin biçimde kullanılması, beyaz gürültüye, yansımalara, kırılmalara ve ekolara karşı dayanıklılık sağlaması amacıyla, elektromanyetik sistemlerde kullanılan modülasyon teknikleri VLC teknolojisine uygulanmasıyla ilgili çalışmalar mevcuttur. Literatürde uyumlu süzgeçlerle verinin alınıp işlenmesi modeli çok sınırlı sayıda çalışmalarda kullanılmış olup, bu çalışmalarda da genellikle LMS algoritmaları kullanılmıştır. Bu tezde, boyutları belirtilmiş dikdörtgen prizma şeklindeki içi boş bir odanın yine sayıları ve konumları belirli, LED'lerden oluşan aydınlatma panellerinden gönderilen verinin foto detektöre ulaştığı ana kadar, kanalın sinyale karşı gösterdiği dürtü tepkisi bilgisayar ortamında farklı FOV açılarına göre analizleri yapılmış, daha

sonra bu belirli FOV derecelerine göre değişen dürtü tepkisine sahip kanallardan veriler alıcıya gönderilmiş, alıcıda işlenen veri, uyumlu süzgeçlerden geçirilerek, bit hata oranı başarımları bilgisayar ortamında değerlendirilmiştir. Uyumlu süzgeçte LMS ve RLS algoritmaları kullanılmıştır. Simülasyon sonuçları SNR'a bağlı bit hata oranı değişiminin grafikleri şeklinde oluşturulmuş olup, RLS algoritması kullanılan uyumlu süzgecin LMS algoritması kullanılan uyumlu süzgeçten daha iyi sonuçlar verdiği gösterilmiştir.

Anahtar Kelimeler: Görünür Işıkla İletişim, Denkleştirici, LMS, RLS

Acknowledgements

I would like to thank my thesis advisor Prof. Dr. Erdal Panayırcı for his kind support, assistance, and patience during my thesis. Without his guidance, it would be impossible for me to finish this thesis.

This master thesis is supported by COST-TÜBİTAK under the project number 113E307.

Table of Contents

List of Tables

List of Figures

List of Abbreviations

AC	Alternating Current
ANN	Artificial Neural Network
BER	Bit Error Rate
CIR	Channel Impulse Response
DFE	Decision Feedback Equalizer
FBF	Feed-Back Filter
FEC	Forward Error Correction
FFF	Feed-Forward Filter
FOV	Field of View
IM/DD	Intensity Modulated Direct Detection
ISI	Inter Symbol Interference
LED	Light Emitting Diode
LMS	Least Mean Square
LOS	Line Of Sight
LTE	Linear Transversal Equalizer
OOK	On Off Keying
OWC	Optical Wireless Communications
PWM	Pulse Width Modulation
RF	Radio Frequency
RGB	Red, Green, Blue
RMS	Root Mean Square
RLS	Recursive Least Square
SNR	Signal Noise Ratio
VLC	Visible Light Communication

CHAPTER 1 INTRODUCTION

Before the discussion moves to the communication by visible light, it is important that we understand currently used communication technologies. Before all else, a definition of communication can be made as the transmission of information from one place to another. The communication method could be via cable or wireless. Communication technologies could employ typical copper cables, CAT5, CAT6 category cables and most popularly fiber-optic cables as the medium. On the other hand wireless communication technologies use air instead of cables as the information transmission medium. Your mobile phone, laptop computer, wireless keyboard/mouse set, wireless earphones and similar devices all transmit information by identification of changes in the electrical field (or in connection with this the electromagnetic field) on the other side (receiver).

Optical Wireless Communications (OWC) is a newly developing technology that provides the media for wireless communication by using infrared, visible or ultraviolet frequencies. Visible Light Communication (VLC) systems on the other hand is a technology that provides wireless communication by using Light Emitting Diode (LED) in visible light frequency with great economic potential. In other words, VLC is the name for a new communication technology that would support the communication currently taking place at radio frequency (RF) band. Visible Light Communication technology is based on transmitting information between two or

more points by using light in the light band visible to the eye. That is to say, it is possible to carry out activities such as going on the internet, holding voice or video calls, watching videos by means of visible light communication technology. VLC, which operates on optic bands and does not require a license for use and has high bandwidth but low costs, has shown itself to be a complementary element in some applications while being a strong alternative in others existing wireless communication technologies.

In traditional radio communication, due to the excessive increases experienced in the fill factor of the frequency spectrum, recently significant difficulties have been encountered in electrical wireless communication technologies. An alternative solution to this is the visible light communication. The subject of communication in visible light band that has a wide and unregulated frequency spectrum has been intensely researched and become the focus of development studies in recent years. Some studies regarding infrared light and laser systems that are the premises of visible light communication and wireless optic communication are currently still in progress. However, generally due to restrictions such as the procurement and cost or the necessary materials, the eligibility of the environment and similar, widespread use has not been possible by the final users. The wireless optic communication handled by using the wavelengths on the visible band of electromagnetic spectrum is a solution to these problems. The ease of procuring the receiver and transmitter resources that are used in Visible Light Communication, which is a type of optic communication whereby the wavelengths in visible band are used, and their lower costs as well as their use for illumination and reaching high data speeds with the communication techniques used make widespread use of VLC systems for wireless optic communication.

The specifications of the LEDs used for VLC technology renders the systems using this technology popular. The longevity and low energy consumption of LEDs provides advantages in comparison to the other light sources. The simultaneous realization of illumination and communication functions results in VLC Systems to have a wide field of use. The LEDs that are used in the illumination of the interiors of offices can also be used in intra-office wireless communication. It is known that the Visible Light Communication besides being used among the vehicles in traffic can also be used for communication inside trains and airplanes [1].

Within the scope of this dissertation, the VLC systems have been discussed, which provide the means for wireless communication by using LED in visible light frequency, which has great economic potential where OWC is concerned. Thanks to its superior properties and wide field of use VLC has the potential to achieve a breakthrough in the area of wireless communication and the developments in this field have been predicted to lead to great changes in the wireless market that is presently dominated by RF technologies. The long-term vision of our country to become the center of production in Eurasia in medium and high technology products could prove to be very profitable for the economy as the R&D activities that would set the stage for commercialization in the field of VLC are performed, VLC technologies oriented to differing wireless applications are developed, and VLC system products by using these are realized [2]. Although there are presently systems working on VLC in the world, these are not able reach the speed of RF systems. With VLC, fast communication can only be possible in enclosed environments. To achieve this improvement some signal processing techniques that increase the data speed are being implemented. One of these methods is to use Adaptive Equalization.

These are methods that are well known in Least Mean Square (LMS) and Recursive Least Square (RLS) literature to ensure filter adaptation [3]. By using these methods the communication speed of VLC could be brought up to GBit/s levels. In our country research studies on the subject are being carried out by limited number of universities and companies. By means of this dissertation it has been aimed to accumulate knowledge in the field of communication with visible light, modeling of channels for VLC Systems that can be used in different environments and increasing the speed of the channel that has been modeled, by using different adaptive equalizers.

1.1 Visible Light Communication

Light radio signals exist in electromagnetic spectrum that contains signals such as the x-rays. The light is the only type of luminescence that is visible among electromagnetic rays.

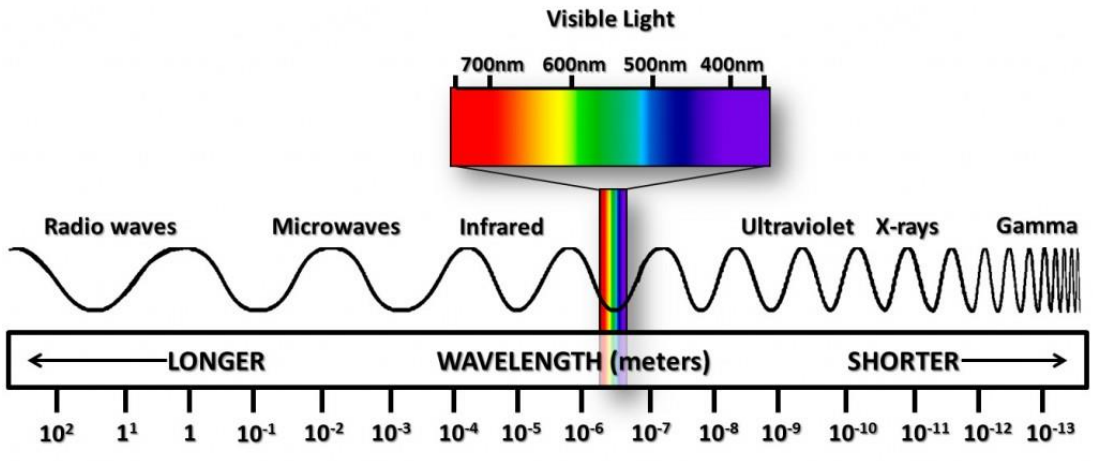

Fig 1.1 Place of the visible light in the electromagnetic spectrum

The wavelength of visible light is in a range of 375 nm – 780 nm. Visible Light Communication is conducted by LEDs that are used for illumination at wavelengths between 375 nm and 780 nm. When we look at the system in terms of the wave width, we see that the communication bandwidth is approximately 400 THz wide. The place of Visible Light Wavelengths in electromagnetic spectrum is shown in Figure 1.1.

When we separate visible spectrum in terms of colors, a separation for colors in following ranges could be observed; Purple color 380 - 450 nm, Blue color 450 - 495 nm, Green color 495 - 570 nm, Yellow color 570 - 590 nm, Orange color 590 - 620 nm, and Red color 620 - 750 nm. By using this information it is possible to use a transmission band range in relation to the color of the light the LED radiates. LEDs differ according to the use of the colors in the visible spectrum. There is a diversification in the form of; RGB (red, green, blue), and phosphor based white LEDs. Besides LEDs, Photo detectors are also important due to the fact that they are used as receiving sources.

VLC, in a similar manner to the other wireless optic communication technologies, takes Intensity Modulated Direct Detection (IM/DD) channels as the basis. When we mention IM/DD it is about the circuits whereby electrical-optical transformations take place as shown in Figure 1.2. Instantaneous optical density i(t), is modulated in direct proportion to the input signal, x(t). This density modulation is performed by the LED lamps in visible light communication. After the modulation, data is transmitted via density signal channel. The photo diode that is available as the photo detector in receiver, transforms the received optic intense signal into electrical current y(t) after detecting it.

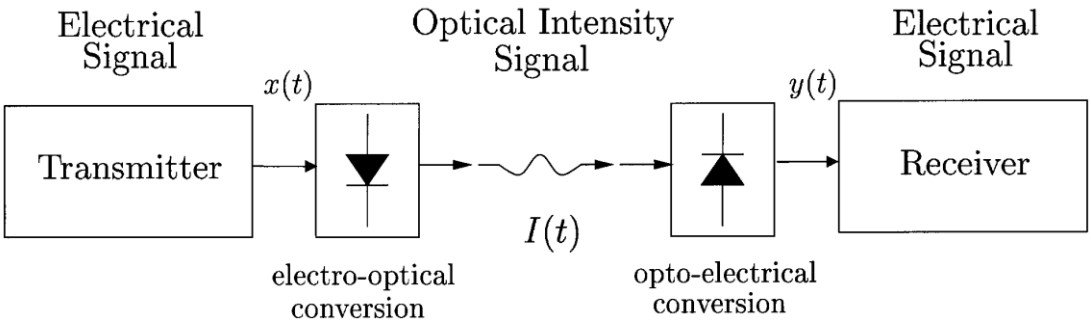

Fig 1.2 Block Diagram of Intensity Modulated Direct Detection Channel

The light that is emitted from the LEDs that are used for both illumination and communication, reaches the photo detectors either directly or by reflection. When we consider how the light is dispersed at a certain angle we can understand that many signals reach the receiver either directly or by being reflected. The signals sent through dissemination of light can be received by means of connecting the photo detectors to the laptops in an office with internet connection.

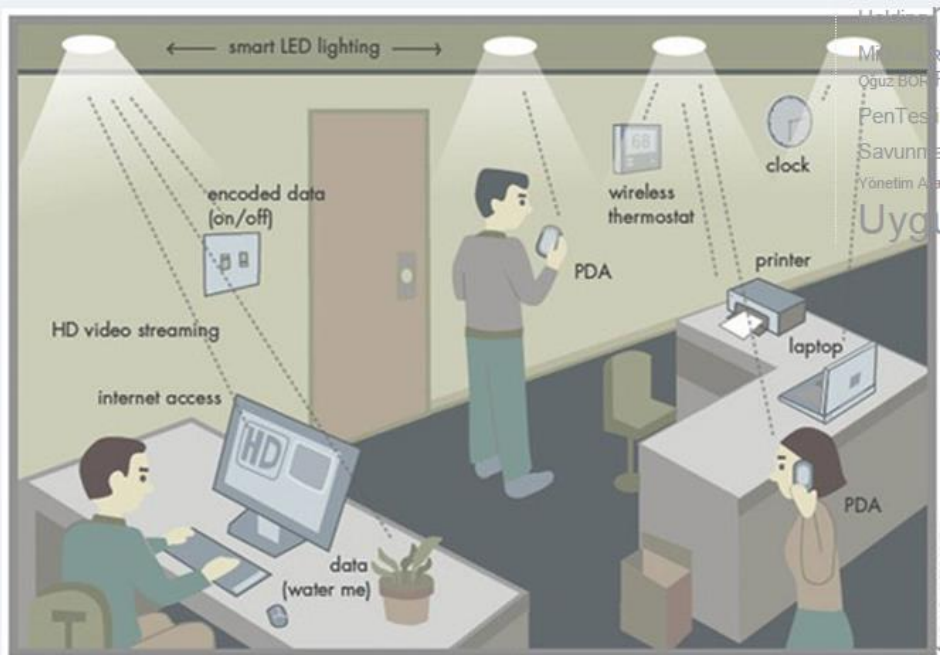

Fig 1.3 VLC Example in Office Environment [4]

Furthermore output requirement could also be met by a direct command to the printer. In the example showing the use of VLC systems in an office environment in

Figure 1.3, the communication provided is one way. For a duplex communication, all sources to be involved in data transmission must be in possession of LED sources. For VLC, the light collected as a result of reflections is also important in addition to the directly transmitted light. The reason for this is the fact that the reflected signals lead to Inter Symbol Interference (ISI). For this reason the delay spread of the channel is required to be known for its characteristics to be determined.

Visible light communication has advantages and disadvantages like RF and IR communications. VLC communication is more advantageous in terms of service and bandwidth in comparison to IR and RF communications. However, in terms of coverage and mobile use, VLC has some disadvantages where RF communication is concerned. It is possible to render the indoor use of VLC, where suitable illumination is available, more attractive by some improvements. Considered from this perspective, there are many areas of use. The fast paced development of VLC has been in progress and as such it has started to take place of RF technology in indoor environments. The fact that, with this technology, the energy consumption is low and sources could be easily obtained is quite advantageous [5]. Another superior quality of VLC systems reveals itself in health and security field. Due to the use of light as an alternative to radio waves in VLC systems, their effect on the health of humans is negligible. Radio waves have the potential of affecting the operation of, in particular, the medical devices by interference. In communication by visible light such interference does not exist. Radio waves are emitted out from the walls without special protection/insulation. In environments requiring security, this causes a security gap. However, it is not possible for the light cross through a wall and therefore, VLC provides superior security in comparison to radio waves.

1.2 Requirement for VLC Systems

With each passing day the need for data increases exponentially. On the other hand the new technologies try to meet this ever increasing need. To give an example, the latest 4G system implements the repeated use of available frequencies as the mobile demand increases and capacity problems are encountered in the system. In spite of the use of serious algorithms, according to Cisco predictions, global mobile information traffic will be reaching 24.3 Exabyte level in 2019 as shown in Figure 1.4.

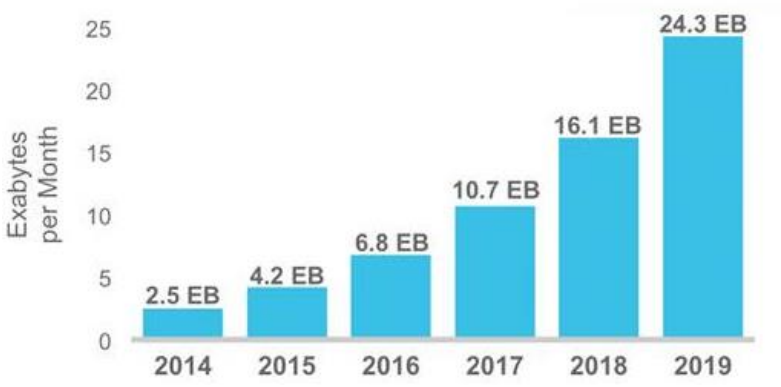

Fig 1.4 Global Mobile Traffic Prediction,[6]

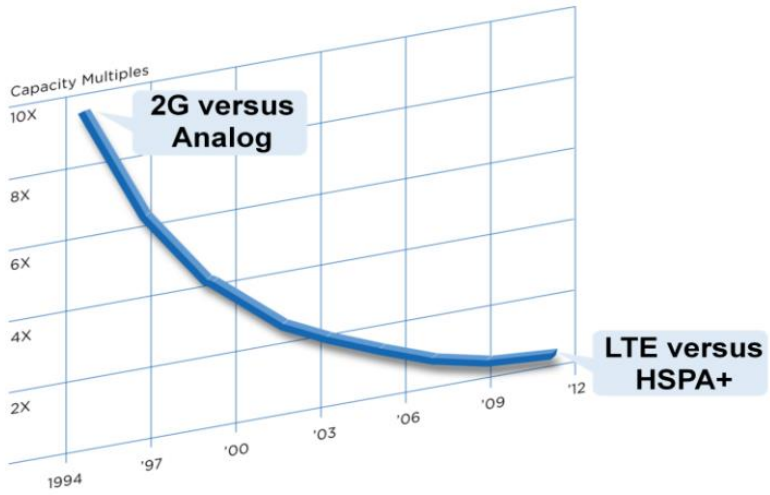

Fig 1.5 Development Coefficient in Spectral Efficiency [7]

When we examine the development graphic of mobile communication technologies shown in Figure 1.5 at this point, we can see that the spectral efficiency development coefficient has been getting smaller since around 2012 and lately it has been observed to approach the theoretical limits. Right at this point in time, the existence of a communication environment that would not act on the radio communication dealing with the ever-increasing mobile demand and decreasing technological efficiency would solve the problem. The most likely candidate for this solution seems to be the VLC technology.

1.3 Visible Light Communication Application Examples

VLC technology has not been developed to fully take place in the existing wireless communication technologies. Its purpose is to be a complementary technology where the available wireless technologies are not sufficient. VLC technology provides a wide field of research and applications. Some of the important applications are as follows:

- **Smart Home Network**

Smart Home Network consists of systems such as sound, data and information communication systems, security-camera systems, air conditioning systems whereby the temperature could be adjusted and similar, integrated on the same centrally managed platform. VLC system provides indoor wireless communication capability including illumination, control and media stream, and internet accessibility that are necessary for the Smart Home Network. This technology reduces the cabling costs and energy consumption in buildings.

- **Mobile Connectivity**

Visible light that is emitted into the environment by LED is redirected to the receiver to achieve secure data transmission. By using this technology it is possible to transmit data at much higher speeds than is possible with wireless communication technologies such as Bluetooth or Wi-Fi.

- **Risky Environments**

In areas where there is the risk of explosion (mines, petro-chemical facilities, oil wells, nuclear facilities, etc.) the communication can be cut off and there could be a problem arising from communication. VLC technology provides safe illumination and wireless communication in risky environments.

- **Vehicles and Traffic**

Current LED lamps are being used on the headlights and internal illumination of the vehicles and traffic lights and streetlights as well. Under the circumstances, it is possible to use Visible Light Communication Technology in establishing communication between the vehicles that get close to each other and the traffic lights to obtain information on the status of the roads and traffic safety applications.

- **Security**

The fact that VLC systems can transmit data securely at high speeds is an important factor to be considered for many applications. The use of visible light provides a great advantage where the security is concerned as the light cannot go beyond the walls surrounding it.

- **Hospitals and Health Care premises**

Use of VLC technology in hospitals and health care premises has great advantages. The use of wireless communication systems such as the mobile phones and Wi-Fi, in hospitals especially close to the magnetic resonance imaging (MRI) devices, in the operating rooms and in some other sensitive areas of the hospital must be avoided. Due to the fact that VLC Technology is light based, it does not have a negative effect on the devices in its peripheral area.

- **Expansion of Wi-Fi Spectrum**

When an established Wi-Fi communication system cannot meet the wireless data requirements, the VLC systems can offer additional bandwidth to be used in the medium concerned. This technology removes RF components and antenna requirement at a low cost.

- **Aviation**

The LED lights providing illumination in planes can at the same time provide media services to the passengers as well as intra-plane communication. As such it could be possible to get rid of the network of cables surrounding the planes. This would reduce of costs of manufacturing planes as well as reducing their weight, which is an important consideration where planes are concerned.

- **Underwater Communication**

Although radio waves cannot be transmitted underwater, visible light could provide high speed data transmission for short distances under the water. By using this property of visible light, the wireless communication between divers and underwater vehicles may be achieved.

- **Sound Applications**

In VLC technology, led lights can be used to achieve wireless sound transmission. Furthermore, numerically different sounds can be transmitted by using different color LED lights.

1.4 The History of Visible Light Communication

In fact, visible light communication using in the human life dates back in ancient time. In this time of history, people carried information for over long distances through the smoke burn fire. Another example can be given lighthouses in terms of providing guidance to the sailors in the later term of history. Most famous of lighthouse was built by Ptolemaic Kingdom in egypt BC 280 and also it is also called The Pharos Lighthouse of Alexandria. Another earliest use of light for communication purposes is attributted to Ancient Greeks and Romans who used their polished shields to send signals by reflecting sunlight during battles [8]. This kind of examples can be given more in the firsth term of visible light communication history. When we come to recent history of the using of light in communication sytems we encounter with the invention of Aleandre Graham Bell's new communication machine it is called Photophone or the alternate name Radiophone. It is very prominent and outstanding invention. The principle of this machine is like that, actually there is no diffrence principally between normal classical telephone and radiophone, photophone was similar to a contemporary telephone but except that it used modulated light as means of wireless transmission while the telephone relied on modulated electricity carried over a conductive wire circuit [9]. In the system it is used that the simplest form of apparatus for producing the effect of a plane mirror of flexible material the back of which speaker's voice is directed. Under the physical

effect of the voice in the air pressure, the plain mirror becomes alternately convex and concave and so and alternately scatters and condenses the light. This was the transmitter part of the system. At the receiver part is used lampblack material but after selenium cell at he focus of a parabolic mirror which is directed to the receiver and this situation is caled in communication Line Of Sight (LOS) position. The cell's electrical resistance varied between 100 ohm to 300 ohm inversely with the falling upon it, its resistance was higher when dimly lit, lower when brightly lit. Finally signal is transformed to electrical energy from optical energy and is send to speaker, and so is obtained the sound again. These examples and explanations are given above to give information for indicate how visible light communication technology evolved in the human history.

More recent work for using LEDs to transmit data by visible light began in 2003 at Nakagawa Laboratory, in Japan. Since then, at Oxford University, there have been numerous research activities focussed on VLC, notably by Smart Lighting Engineering Centre. Today, the VLC standardization named as 802.15 by IEEE Wireless Personal Area Networks working group.

1.5 Literature Review

White LEDs used indoor visible light communication system is proposed in [10]. In this research, the LEDs are used both illuminating and optical wireless communication receiver. On-off Keying Return-to-Zero (OOK-RZ) coding is used for modulating. Optical lighting and optical transmission have been tested to evaluate the requirements for indoor applications. They presented that the effects of the delay problems faced in the high data rate transmission [10]. LEDs are also being used in

traffic for communication. In [11], road-to vehicle communication in the traffic signal lights by using the LEDs was proposed. In this research, they used a camera on the front end of the car. The camera is used for receiving information from traffic signal lights. The advantage of proposed system is multiple data can be transmitted by the LEDs and received by high-speed cameras [11]. Using the existing power-line for optical communication in a household is proposed in [12]. The power-line is used for communication between white LEDs and other networks. The also used power-lines and outlets behave as data networks and ports. The transmitted signals are added to the cyclic waveform of the alternating current (AC) for optical intensity modulation. The transmitter signal from the PC is picked through the power-line, and biased before sending to the optical receivers. So LEDs are converted the electrical signal into an optical signal. After that signals sends it to the photodiode, where it converts the captured optical signal to an electrical signal. The signal is demodulated according to the received level of light and then is sent to the mobile terminal [12]. Optical communications for outdoor communication has been discussed in [13]. Laptops and mobile phones can be used for transmitting and receiving information, using transceivers. Both LEDs and photodiodes are used as transceiver systems. To reach the most viable modulation, intensity modulation was implemented [13]. The example of VLC system in wireless underwater communication was proposed in [14]. They used VLC for robotic inspection of nuclear power plants. They also explained the solution for maintaining the consistent line of sight to maintain a communication link in detail in [14]. In this research, an optical wireless network was used between the remotely operated vehicles and control station using LEDs and photodiodes on both sides. Underwater remotely operated vehicles was used to communicate with the control station over water to transmit control signals. Both the

control station and vehicle are able to directing a light beam in the three-dimensional space [14]. In [15], researchers designed a prototype to demonstrate VLC using RGB LEDs and sensors. The RGB LEDs enable parallel signal communication. They also used microcontroller to control them. To switch RGB LEDs at high speeds, they used Pulse Width Modulation (PWM). To realize multiple value signals communication, the characteristics of the variation in color and change in intensity of LEDs was analyzed [15]. In [16], researchers proposed a VLC system to transmit high quality video and audio signal. The video signal was modulated by using a high speed comparator in the transmitter. The analog signal was converted from analog to digital. Signals were transmitted using the illumination LEDs in the transmitter. They also used photodiode as the receiver for sensesing the optical signals and photodiode also converted optical signal into electrical signals. The electrical signal is then amplified and converted back to video/audio out [16]. A different design was proposed in [17] for an ultra-thin secondary lens by using white surface mount device LEDs for VLC. The blue LEDs are used as receiver and they were mounted directly on the surface of the mobile device. The precise modeling of the system was analyzed and verified.

In [18], they proposed an indoor visible light wireless communication system that utilizes multiple white LED lighting equipment. While the number of sources permits site diversity transmission over LOS links, the optical path difference between the multiple sources triggers intersymbol interference, which significantly degrades system performance. They overcomed the ISI problem by proposing an adaptive equalization system. They elucidated the most effective training sequence interval for channel estimation in a mobile environment. And they showed that the adaptive equalization system with the effectual interval alleviates the influence of

shadowing [18]. In paper [19], researchers proposed LED panel model that can place LEDs with some angle. Based on the simulation results, the effect of changing LED directions is analyzed and the optimal direction of LED is pointed out. Reduced training sequence in a Decision Feedback Equalizer (DFE) with RLS adaptive algorithm to mitigate the effect of ISI in an indoor Visible Light Communication channel presented in [20]. They analyzed the performance of the RLS algorithm with the DFE for the improvement of bit error rate (BER) in an indoor channel model. According to [20], they have proven that with the proposed RLS equalizer, the training sequence can be reduced to allow more data bits to be transmitted for the identical BER performance. In reference [21], they experimentally demonstrated for the first time an on off keying modulated visible light communications system achieving 170 Mb/s using an artificial neural network (ANN) based equalizer. In that research, Adaptive DFE and linear equalizers were also implemented and the system performances were measured using both real time and offline implementation of the equalizers. The performance of each equalizer was analyzed in [21] using a low bandwidth light emitting diode as the transmitter and a large bandwidth photodetector as the receiver. The achievable data rates using the white spectrum were 170, 90, 40 and 20 Mb/s for ANN, DFE, linear and unequalized topologies, respectively. Channel modeling for visible light communications using ray tracing approach was investigated [22]. The simulation environment was created in Zemax® and enabled us to specify the geometry of the environment, the objects inside, the reflection characteristics of the surface materials as well as the specifications of the light sources and receivers. The received optical power and the delay of direct/indirect rays were computed for the specified indoor environment and the corresponding channel impulse response (CIR) is obtained through proper

normalizations. They presented CIRs for a number of indoor environments and quantify multipath channel parameters gain for each environment [22]. Simulation program for indoor visible light communication environment based on MATLAB and Simulink was reported in [23]. The program considers the positions of the transmitters and the relections at each wall. For visible light communication environment, the illumination light-emitting diode was used not only as a lighting device, but also as a communication device. Using the simulation program, the distributions of illuminance and root-mean-square delay spread are analyzed at bottom surface [23]. Gigabit-class indoor visible light communication system using commercially available RGB White LED and exploiting an optimized modulation were realized experimentally [24]. They achieved data rate of 1.5 Gbit/s with single channel and 3.4 Gbit/s by implementing transmission at standard illumination levels. In both experiments, the resulting bit error ratios were below the Forward Error Correction (FEC) limit [24]. In [25], they presented experimental results demonstrating a higher than 100 Mb/s visible light communications system using linear adaptive equalizers. In order to achieve high transmission speeds, generally the research community has adopted spectrally efficient modulation formats such as discrete multi-tone and equalizers were overlooked. The reason for that was unclear as equalizers offer a substantial capacity for removing inter-symbol interference. As a result, they implemented a line-of-sight VLC link with an ~8 MHz bandwidth and a linear feedforward equalizer; the number of taps was varied in order to gain insight into the system performance using varying complexity. The 120 Mb/s transmission speed ultimately achieved offers a bit-rate to bandwidth gain of ~15 times [25]. The lighting levels within the VLC area was simulated for different configurations of LED placement ın [26]. Furthermore, various network topologies like linear-bus,

star, and tree were experimented. It was observed that star network uniformly distributes the signal to all the LEDs and offers higher signal to interference ratio. Following the results of [26], star distribution network for the chosen LED placement scenario will be implemented. The aim of research in [27] was the evaluation of spectrally efficient optical wireless transmission techniques in indoor environments. They analysed the potential of the parallel usage of several optical transmitters. It is found that the usage of multiple optical transmitters and receivers could substantially improve the performance of OWC. A novel transmitter concept for OWC was also proposed in [27].

1.6 Contribution and Organization of Thesis

In this thesis, a visible light communications system operating in an empty room with rectangular prism shape and certain dimensions is designed and analyzed both theoretically and by computer simulations. Whole the simulations and analysis algorithms are coded in the scope of this thesis by us. None of the extra program such as Zemax or other simulation programs have not been used in this thesis. The LED panels are placed in numbers and positions on the previously determined locations, which send data (light signal) through the optical channel to the receiver having photo detector to implement optical to electrical conversion. The impulse response displayed by the channel through which the data is sent is analyzed and graphed according to different Field of View (FOV) angles by computer simulations. Later on, the data (light signals by means of LEDs) is transmitted to the receiver through these channels that have differing impulse responses based on specific FOV degrees. The data, processed at the receiver, is passed through an adaptive equalizer

to evaluate the bit error rate (BER) performances by computer simulations. Least-mean-square (LMS) and recursive least square (RLS) algorithms are used for the adaptive equalization. The simulation results are presented in graphics of bit error rate (BER) as a function of signal-to-noise ratio (SNR). It is concluded that the adaptive equalizer filter on which RLS algorithm is employed provides better performance results than the adaptive equalizer filter realized by the LMS algorithm.

In the "Introduction" Chapter of the thesis, the basic definitions related to VLC are provided, the advantages and disadvantages of the technology are introduced and the summary of the literature covering the recent years is provided. The second chapter is reserved for background theories on visible light communications (VLC). In this chapter explanations pertaining to the following are provided in the order they appear;

- Structure of LEDs,
- Structure of photo detectors,
- Dissemination of light, channel modeling for VLC and adaptive equalization.

The third chapter of the thesis introduces the simulation environment realized and the program implemented to realize the subject matter simulation within the scope of the thesis. In the fourth and the last chapter titled "Test and Results", the results of the study and their interpretations are provided.

CHAPTER 2 BACKGROUND THEORY

In this chapter, some basic subjects are discussed that would aid us in explaining the study conducted within the scope of the thesis. These subjects in the order they appear are; structure of the LEDs that are used as transmitters in VLC systems, structure of the photo detectors used as receivers, dissemination of the light carrying the message sent by the transmitter in the environment, channel modeling for VLC and adaptive equalization implemented to improve the speed of communication.

2.1 Light Emitting Diode

LED (Light Emitting Diode) is a semi-conductor, diode based, light emitting electronic circuit element. LED, whose electrons are mobilized by means of the applied current and start emitting light. This effect is named electro-luminescence and it was discovered in 1907 British researcher H.J. Round. The first commercial purpose LEDs were used as only low density red colored light sources in place of incandescent and neon indicator lamp. Initially they were used in expensive devices such as laboratory and test equipment and later on to provide visual experience in devices such as TVs, radios, calculators, etc. The light output value of LEDs has developed in line with the improvements in material technologies. The researching

and development of high power white light LED made the use of LEDs in the field of illumination. Presently, LEDs could be in colors of high shine, extending along the visible section between the ultraviolet and infrared wavelengths. On the other hand the composition of the chemicals used determines the color of the light. LEDs have a series of advantages in comparison to the traditional sources of light such as the low energy consumption, longevity of product, durability, small size and fast switching on and off capability. However, they are slightly more expensive than those technologies.

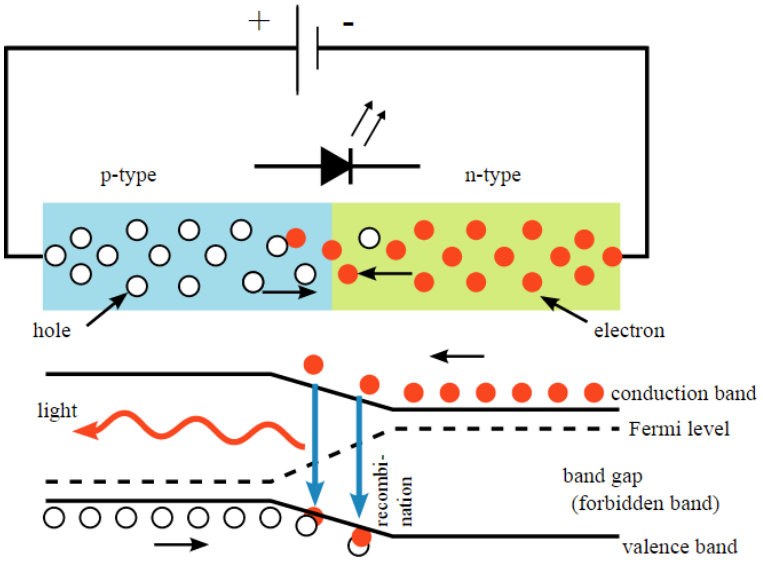

Fig 2.1 LEDs and working principle[28]

The operating principle of LEDs and their presentation in the electronic circuit are shown in Figure 2.1. When LEDs are polarized in the direction of the transmission the free electrons pass through P-N junction and enter into P section. Some of these merge with the holes here. The energy that is revealed as a result of this merge is in the form of light energy. The value of the current flowing through P-N junction is dependent on the number of the electrons and holes. According to the quantum theory, light energy is created as a result of the merging of electrons with the holes. The amount of the energy revealed here depends on the width of the P-N passage.

Although every color can be produced by LEDs within the visible region, white light is the most desirable color for general illumination. White light emission from an LED is by mixture of multi-color LEDs or by the combination of phosphors with blue/UV LED emission [29]. There are different types of white LEDs. Some of the important ones are Phosphor based White LEDs, Ultraviolet (UV) based White LEDs and RGB (Red-Green-Blue) LEDs.

2.1.1 Phosphor based White LEDs

Phosphor based LEDs emit light with less illumination efficiency (<80 lm/watt [30]) than RGB LEDs. But on the other hand it has advantages like being created from a single color, cheaper provision in comparison to RGB LEDs and being less complex in nature. The band width has been increased to 20 MHz level by using "Blue Filtering", an optical technique [31]. Only one color LED is being used in phosphor based white LEDs. When the illumination density of phosphor based white LEDs is examined against their wave length, it can be observed that the blue light provides higher density illumination as can be seen from Figure 2.2.

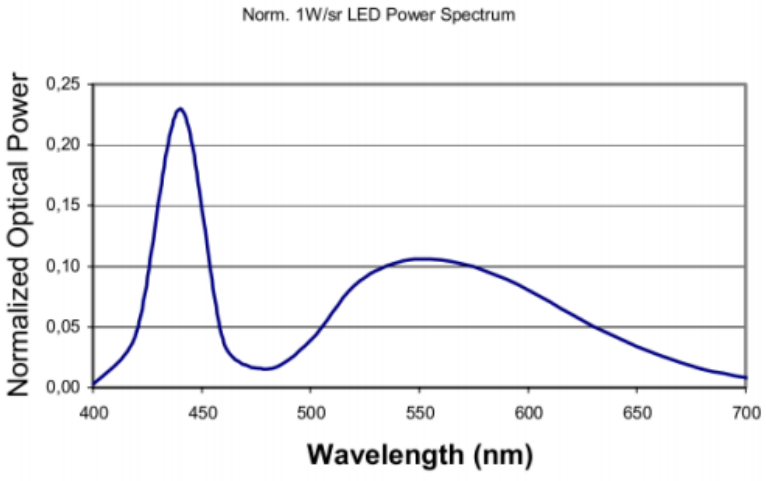

Fig 2.2 Normalized optical spectrum of a white LED [32].

2.1.2 Ultraviolet based White LEDs

Ultraviolet LEDs were fabricated with pre-coating blue/green/red phosphors onto ultraviolet (UV) LED to emit white light [29], [33].

2.1.3 RGB LEDs

An RGB 3-chip LED is a mixture combination of three colors to produce white light with little variance in the Kelvin color temperature [34]. What we see coming from the sun is white light. We know that the visible spectrum of radiation that the sun emits is actually a broad range of wavelengths, ranging from red to orange, yellow, green, blue, indigo to violet. When this broad range of colors impinges on our retina, our brain interprets it as "white". A tri-color LED tries to mimic this effect by outputting a board range of wavelengths. Note that the three dominant wavelengths of the tri-color LED are at the ends and the center of the visible spectrum, thus attempting to replicate the coverage of the range and getting close to as possible (with minimal hardware). So, it is less of a mixing and more of an attempt to create a continuous function by using a few sampled points.

2.2 White LEDs as a Powering and Lightening Element

Visible light communication at the same time contains the elements that are used for illumination. When illumination takes place, the switching operations due to communication, in other words switch on and offs must be realized very fast as the frequency at which the human eye perceives a change is approximately around 200

Hz [35]. Therefore, the change that could not be perceived by human eye must take place in less than 5 milliseconds. To be able to achieve correct illumination the properties and positions of the illumination elements must be determined accurately. The properties defining a LED can be listed as follows; optical power P_t, luminous intensity in accordance of normal vector $I(0)$ and semi-angle at half luminance $\phi_{1/2}$

Energy flux in other words the emission spectrum of the LED used is shown by Φ_e. An example for phosphor based white LED energy flux function is provided in Figure 2.2. The integral of Energy flux value in all directions give optical power P_t, value with units measured in watts and it is calculated as shown in Eq.2.1.

$$P_t = \int_{\Lambda_{min}}^{\Lambda_{max}} \int_0^{2\pi} \Phi_e d\theta d\Lambda \tag{2.1}$$

The $\Lambda_{min}$and Λ_{max}values used in this equation shows the energy flux function limits of the subject matter LED. In other words it shows the limits in which the LED could generate energy.

Luminous flux Φ, with units in Lumen (lm) and defined as the illumination flux, is calculated as shown in Eq. 2.2.

$$\Phi = K_m \int_{\lambda_{min}}^{\lambda_{max}} V(\lambda)\Phi_e(\lambda)d\lambda \tag{2.2}$$

In this equation $V(\lambda)$ is the standard eye sensitivity function [36]. This function that is also known as the illumination efficiency curve is in the shape of an inverted bell whereby it reaches its maximum value at $\lambda = 555\ nm$ and diminishes in value as we move along the curve in both directions. The K_m value shows maximum visibility value and as such it has been determined to be approximately 683 lm/W in experimental studies. It is used as a fixed value. This value is naturally obtained at 555 nm wavelength.

Luminous intensity (I) is the amount of visible power per unit solid angle (Ω), measured in candelas (cd) and calculated by Eq. 2.3.

$$I = d\Phi/d\Omega \tag{2.3}$$

It is considered that a uniform point light source would emit the same amount of luminous intensity in each direction. However, in application this is not the case. To give an example, while any LED emits the highest luminous intensity in line with what is normal for it, this value gets smaller as we move farther away from the normal. The luminous intensity value that a LED gives in the direction that has ϕ degrees angle difference with the normal of that LED is shown in equation Eq. 2.4.

$$I(\phi) = I(0)cos^{m}(\phi) \tag{2.4}$$

The $I(0)$value used in this equation is theluminous intensity value the LED provides in the direction of its norm and it is a quality specific to the LED used. Order of Lambertian emission on the other hand indicated by$m$value and is calculated as shown in Eq. 2.5.

$$m = -ln(2)/ln\left(cos\left(\phi_{1/2}\right)\right) \tag{2.5}$$

The $\phi_{1/2}$value used in this equation is named as semi-angle at half luminance and is again a quality of the LED used. Order of Lambertian emission theoretically takes on zero value for ideal point light source that emits equal intensity light in each direction. Under the circumstances $I(\phi) = I(0)$ equality occurs in Eq. 2.5.

Luminous intensity (E) defined in lux (lx) in terms of units, is defined as the amount of light falling onto a point and calculated by means of Eq. 2.6.

$$E = \frac{d\Phi}{dA} = \frac{d\Phi}{r^2 d\Omega} = \frac{I(\theta)}{r^2} \tag{2.6}$$

The Ω symbol used in the equation indicates the spatial angle while r symbol shows the distance between the receiver and transmitter.

2.3 Photodiode

For the communication infrastructure to be established, the specifications of photodiodes as receiving sources are as critical as the LEDs that are the transmitting sources in visible light communication. Photodiodes are solid state elements that convert optic signal into electrical signal and their representative form is provided in Figure 2.3 [37]. The electric current that is generated from the optic signal that reaches the photodiode itself, is used to extract the information transmitted.

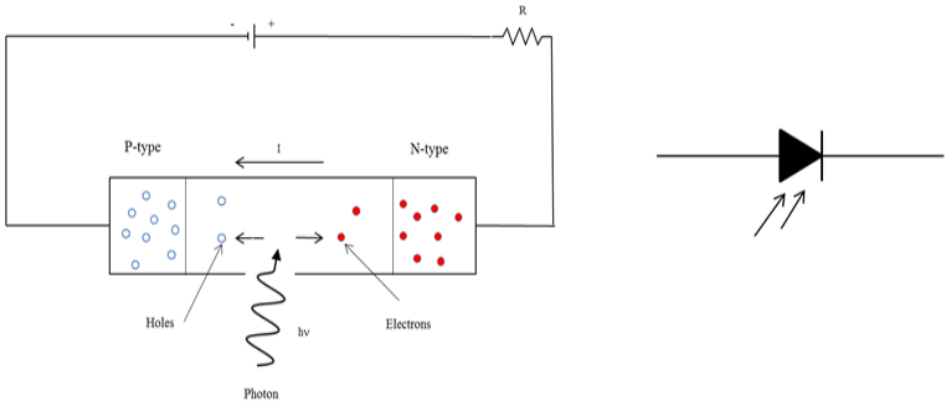

Fig 2.3 Basic biasing arrangement and construction and Circuit symbol representation of photodiode [37]

A photodiode is defined by means of the convergence efficiency (γ), Field of View (FOV) (ψ_c), detector physical area (A), gain of an optical filter ($T_s(\psi)$), optical concentrator ($g(\psi)$) and reflective index (n) values. The ψ symbol used in these expressions shows the angle the light makes with the normal of the receiver and defined as the angel of incidence of the light.

Convergence efficiency parameter is a fixed value showing the rate at which photodiode converts the optic power into current or potential difference. None of the photodiodes could catch all the light falling onto it. It can only catch the rays that

display a deviation up to a certain angle with the norm of the receiver. The angle of incidence of the light that the Photodiode could catch at the greatest angle difference with the normal shows the FOV value of that photodiode. This is a fixed value in terms of the photodiode used. When the angle of incidence of the light is greater than the FOV value ($\psi > \psi_c$) it would not lead to any reaction at the receiver. As the physical area, that is the area along which light can be caught, increases the power of the optic signal reaching the receiver it will increase in linear proportion. Physical area value is also a fixed value in terms of the photodiode used. The light entering the optic receiver goes through a transformation depending on the angle it makes with the normal of the receiver. This transformation function is called gain of optical filter. Ideally $T_s(\psi) = 1$ is accepted, meaning none of the angles goes through transformation. In visible light communication, a thin edged lens with reflective index value of *n* is placed in front of the photodiode to increase the area of optical concentrator [38]. This effect leads to an impact in the form of a linear increase in the received optic power value and the subject matter effect is calculated by means of Eq. 2.7 based on the angle of incidence of the light rays.

$$g(\psi) = \begin{cases} \frac{n^2}{sin^2_{\psi_c}}, & 0 \leq \psi \leq \psi_c \\ 0, & \psi > \psi_c \end{cases} \tag{2.7}$$

Instead of using a lens, if the surface area of the photodiodes is enlarged, then the capacity of the photodiode circuit must be increased. This increase would lead to an increase in the noise level in the receiver therefore it is not desired.

When a receiver with P_t power and an ideal point light source of d distance (m = 0) reach the photodiode, which is expressed by means of the symbols above, at angle ψ, the perceived power at photodiode (P_r) is calculated by means of Eq.2.8.

$$P_r = \begin{cases} P_t\, A\, T_s(\psi)\, g(\psi) \cos(\psi) \,/\, (2\pi d^2), & 0 \le \psi \le \psi_c \\ 0, & \psi > \psi_c \end{cases} \quad (2.8)$$

However, LEDs, due to the fact that they behave Lambertian and have an *m* value different than zero, cannot emit light of the same intensity in every direction from the source of light. Under the circumstances, the angle that the light rays exiting the light source make (ϕ) and Order of Lambertian emission (m) value must be taken into account. Consequently the equation takes the form provided under Eq. 2.9. In Fig 2.4 the light rays falling on the LED and photodiode have been shown in representation.

$$P_r = \begin{cases} P_t\, A\, (m+1)\, cos^m(\phi)\, T_s(\psi)\, g(\psi) \cos(\psi) \,/\, (2\pi d^2), & 0 \le \psi \le \psi_c \\ 0, & \psi > \psi_c \end{cases} \quad (2.9)$$

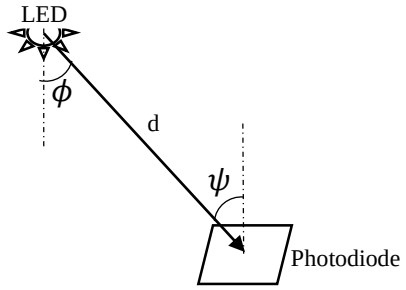

Fig 2.4 Received Power on Photodiode

The optical power received at Photodiode is linearly converted into electrical signal (S_r) as shown in Eq. 2.10 based on the convergence efficiency value of the photodiode.

$$S_r = \gamma\, P_r \quad (2.10)$$

2.4 Propagation of Light

When light illuminates an environment, the rays that affect each point in the illuminated environment are split into two. The first one of these would be the light coming directly from the source that is LOS and the reflections of the light rays that

bounce from another object. Provided that there are no obstacles on the way, only one direct beam (LOS) is received at each point in the environment from each source; however there are also light rays received from infinite number of reflections (bLOS). When light hits a surface and is reflected, it loses some of its energy. Furthermore, due to the fact that the geometry of the surfaces would not necessarily be straight, the signals could be subject to scattering. In literature it is considered that the surfaces would reflect the light they receive according to a certain coefficient. This value, which is named the Reflectance coefficient (ρ), changes according to the surface that is reflecting the light and wavelength. In Figure 2.5, the graphic of change in spectral reflectance values according to the light wavelength of different materials is given. In the analysis of VLC systems, the reflectance coefficient of the reflective surface is considered to be fixed.

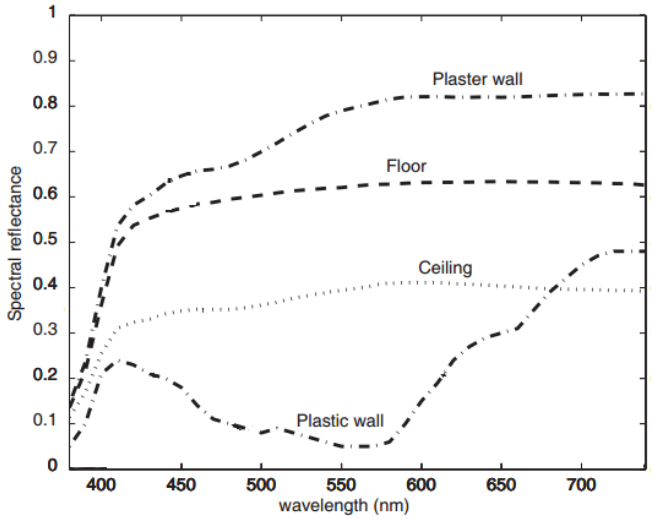

Fig 2.5 Spectral Reflectance values of different materials according to the light wavelength [39]

At any point on the surface where the receiver is located just one light ray is received from any linear light source. If the light ray is received at a right angle, then the illumination power to be generated is determined as per Eq. 2.6.

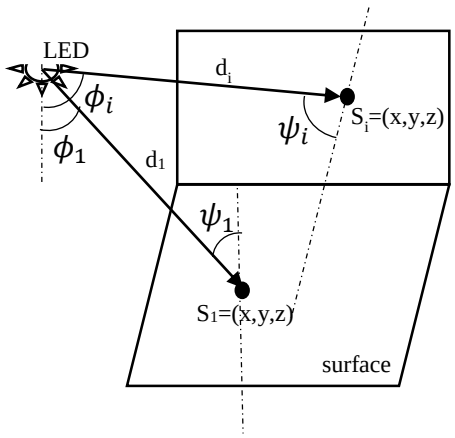

Fig 2.6 Light rays emitted from a single source, falling on one point on each one of the two surfaces at a right angle to each other

As shown in Fig.2.6 the luminance (E_0) of the direct light rays that are emitted from a single light source and fall on a point on two sample surfaces perpendicular to each other at different angles is calculated by means of Eq. 2.11.

$$E_{0,i} = I(0)cos^m(\phi_i)cos(\psi_i)/{d_i}^2 \quad (2.11)$$

In Fig. 2.6 LED has been shown by means of dashed lines in the normal direction of sample point on the horizontal plane and sample point on the perpendicular plane. With Eq. 2.10 only direct illumination can be calculated. Although the most important illumination ray that affects a point would be the direct light ray from the light source, there are also light rays that illuminate another point after leaving the light source and reach the point under analysis after being reflected from their initial destination. In reality there are unlimited numbers of reflections that affect a point. However the luminance decreases due to distances involved in each reflection. In practice, in addition to direct illumination the 1st order reflections are also taken into account in majority of the cases. Under some circumstances 1st and 2nd order reflections are considered. Within the scope of this thesis only 1st order reflections have been accounted for. In Figure 2.7, the representative form of 1st order reflection

is depicted. The illumination point is indicated by S while all the points from which a reflection can fall on point S are indicated by S_w.

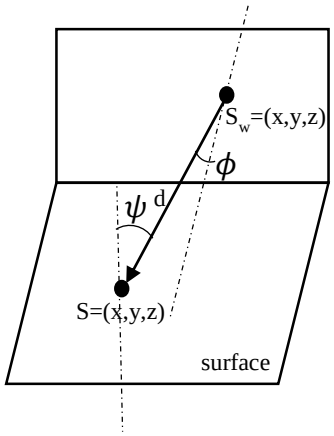

Fig 2.7 1st order reflection

If the angle at which the light coming from any 1st order reflection falls on the point being analyzed is indicated by ψ, the exit angle from the point at which the reflection occurs by ϕ, the distance between the surfaces the light is reflected from and to by$d$, the direct luminance at the point of reflection by $E_{0,w}$, reflection coefficient of the surface from which the light is reflected by ρ, surface area with infinitesimal reflectiondA_{wall}, then the luminance from 1st order reflections reflected on point S from all points other than point S itself is calculated by means of Eq. 2.12 in the form of $(E_{1,S})\ n = 1$.

$$E_{n,S} = \int_{wall} E_{n-1,w}\ \rho\ cos(\phi)\ cos(\psi)\ dA_{wall}/(\pi d^2) \quad (2.12)$$

If it is desired to take into account higher reflections then n value is increased. Under such circumstances, the total luminance falling onto an S point is calculated by using Eq. 2.13 below.

$$E_S = \sum_{i=0} E_{i,S} \quad (2.13)$$

The calculation of the optical power received by means of direct illumination at the photodiode at the point of analysis is given in Eq. 2.9. We can state the expression in

Eq.2.13 by changing the variable $P_{r,0}$to be only the optic power from the direct light received so that $P_{r,0} = P_t H_0$ equality can be achieved as indicated in Eq. 2.14.

$$H_0 = \begin{cases} A\ (m+1)\ cos^m(\phi)\ T_s(\psi)\ g(\psi)\cos(\psi)\ /\ (2\pi d^2), & 0 \le \psi \le \psi_c \\ 0, & \psi > \psi_c \end{cases} \quad (2.14)$$

Optical power is also channeled to the photodiode by means of reflections as in the case of the luminance. Eq. 2.15 is used to calculate only the optical power caused by the 1st order reflections.

$$P_{r,1} = \int_{wall} P_t\ H_1 dA_{wall} \quad (2.15)$$

H_1in this expression is calculated by means of Eq. 2.16.

$$H_1 = \begin{cases} \rho A(m+1)cos^m(\phi)T_s(\psi)g(\psi)\cos(\psi)\cos(\alpha)\cos(\beta)\ /\ \left(2\pi {d_1}^2 {d_2}^2\right), & 0 \le \psi \le \psi_c \\ 0, & \psi > \psi_c \end{cases} \quad (2.16)$$

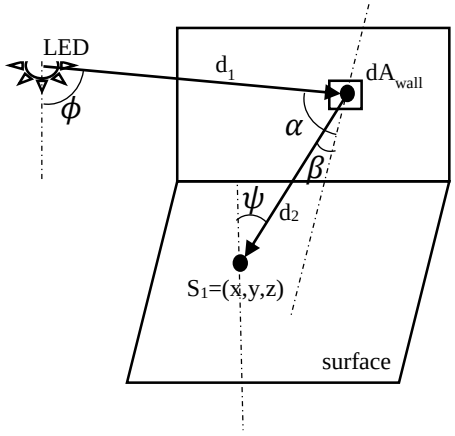

Fig 2.8 Demonstration of the optical power produced by 1st order reflection

In Eq.2.16, surface reflection coefficient has been expressed by ρ, the angle of the light bean from the light source to the surface that it will be reflected from by ϕ, the angle at which the light beam reaches the reflection surface α angle at which the beam leaves the reflection surface byβ, the angle at which it reaches the photodiode by ψ, surface area with infinitesimal reflection by dA_{wall}, distance between the light source and the reflection surface by $d_1$and the distance between the reflection surface and photodiode by d_2. The symbols used are shown in Figure 2.8. Under the

circumstances, the total optical power that is generated in the photodiode by the light caused by directly received beams as well as the 1st order reflections is calculated by means of Eq. 2.17.

$$P_r = P_{r,0} + P_{r,1} \tag{2.17}$$

2.5 Channel Model

The channel structure in visible light communication shows a similarity to the other IM/DD channels. Determination of the channel structure as well as the channel impulse response will help generation of ideas prior to the improvements in both the receiver and transmitter. When the example provided under Figure 2.9 of VLC communication infrastructure is examined it can be observed that the optically dense signal ($X(t)$) that is emitted from LED lamps, which are transmitter sources, pass through the channel ($h(t)$) and gathered together with the noise signal ($N(t)$) at the receiver, electric current forms at the receiver signal ($Y(t)$).

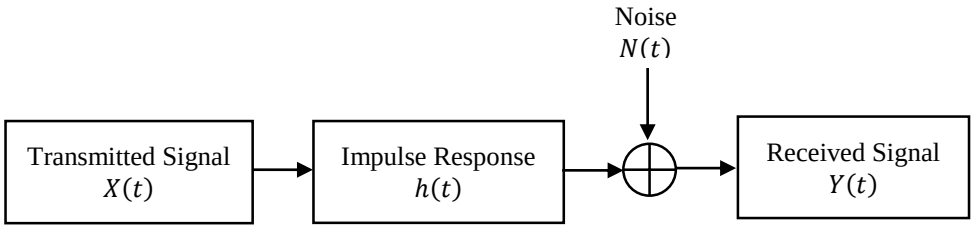

Fig 2.9 Visible Light Communication Channel Model

The VLC channel model is shown below by means of Eq. 2.18, whereas convergence efficiency of photodiode element is shown by γ.

$$Y(t) = \gamma X(t) \otimes h(t) + N(t) \tag{2.18}$$

Knowing the channel model and the impulse response ensures that the analysis of the signal coming to the receiver could be done more accurately. Many studies have been conducted for the modeling of the channel and determination of the impulse response. According to Ray Trace simulation model all light beans reaching the receiver either directly or by means of reflection would reach their targets with some shifts in time depending on the distance they cover. All light beams would not be able to reach the receiver and thus there will be some distortions in impulse response. Especially the light beams that reach the receiver later than symbol period will cause an effect in the next symbol's time period. This distorting effect is named intersymbol inference (ISI). The impulse response of VLC system is calculated by using Eq. 2.19 as number of all light beams [22], both direct and reflected, reaching the receiver point is expressed by N_r, the power that the beams generate at the receiver by P_i, time necessary for the light beams to reach the receiver byτ_i, and Dirac Delta function by $\delta(t)$.

$$h(t) = \sum_{i=1}^{N_r} P_i \delta(t - \tau_i) \quad (2.19)$$

2.5.1 Mean Delay and Root Mean Square Delay Spread

The root mean square delay spread term for the channel has widespread use to determine the distribution properties of multiple track channels. Root Mean Square (RMS) delay spread that occurs for the only optic source in VLC communication, is lower in comparison to infrared optic communication [40] due to the low amplitude of the reflected signals in VLC Communication in comparison to infrared optic communication. When we examine the channel models we see that multiple track signals reach the receiver in communication with nLOS channel. This situation

requires that the time distribution properties of the channel are known. RMS delay spread provides the time distribution information of multiple track channels. If RMS delay spread is large, coherence bandwidth of the channel decreases and the channel frequency is converted into a selective structure. However, if RMS delay spread is low, phase coherence bandwidth of the channel increases and the channel frequency is converted into a proper structure.

The average delay spread of the channel is calculated by means of Eq. 2.20 before RMS delay spread.

$$\tau_0 = \frac{\int_{-\infty}^{\infty} t\, h^2(t)dt}{\int_{-\infty}^{\infty} h^2(t)dt} \tag{2.20}$$

On the other hand RMS delay spread is calculated by means of Eq.2.21.

$$\tau_{RMS} = \sqrt{\frac{\int_{-\infty}^{\infty}(t-\tau_0)^2 h^2(t)dt}{\int_{-\infty}^{\infty} h^2(t)dt}} \tag{2.21}$$

2.5.2 Channel Noise

Due to the fact that visible light communication is based on the density of light, the light density occurring in the background also reaches the receiver causing noise. The source of this type of noise that is called background noise, and could be a natural or artificial light source [41]. For indoor spaces, sunrays may not be a direct source of noise however, light sources such as the fluorescent, incandescent illumination and candles cause background noise signal to reach the receiver in indoor environments. These signals that reach the receiver generate DC current at the photodiode. The noise that the generated current causes is called shot noise [42]. These noise signals reaching the photodiode display Poisson distribution. The subject matter noise signals are independent from each other and when they are collected at

the receiver their distribution would be in Gauss distribution. In addition to shot noise there is also thermal noise caused by load resistance at the receiver. These two noise types are independent from each other and as such the noise of the channel could be expressed by using Eq. 2.22.

$$\sigma_{noise}^2 = \sigma_{shot}^2 + \sigma_{thermal}^2 \quad (2.22)$$

In channel model, N(t) that is defined as the noise at t moment is a random value chosen from Gaussian distribution in possession of σ_{noise}^2variation.

2.6 Filters Used in VLC Systems

Many communication channels including telephone channels, some radio channels and visible light communication channels are considered to have band-limited linear filter structure. To be able to achieve distortion free transmission, within the frequency band used by the signal transmitted, the amplitude response of the channel $A(f)$ must be fixed while phase response $\theta(f)$ is linear with frequency. When the fact that the amplitude response of the channel is not fixed, channel amplitude distortion occurs and when the phase response is not linear, channel phase distortion (delay distortion) occurs. Most communication channels like VLC system distorts the signal transmitted thus the resolution of the information at the receiver becomes difficult and errors occur. To remove any effects arising from the inferior frequency response of the channel and to be able to provide better resolution (at demodulator) some special filters or equalizers are used. Under the sub-headings of this thesis, Raised Cosine Filter and Adaptive Equalization filtering techniques used in the receiver will be discussed.

2.6.1 Raised Cosine Filter

A communication channel in possession of limited bandwidth and linear phase response, affects a rectangular impulse sent by On Off Keying (OOK) Modulation , in time and frequency domain as shown in Figure 2.10.

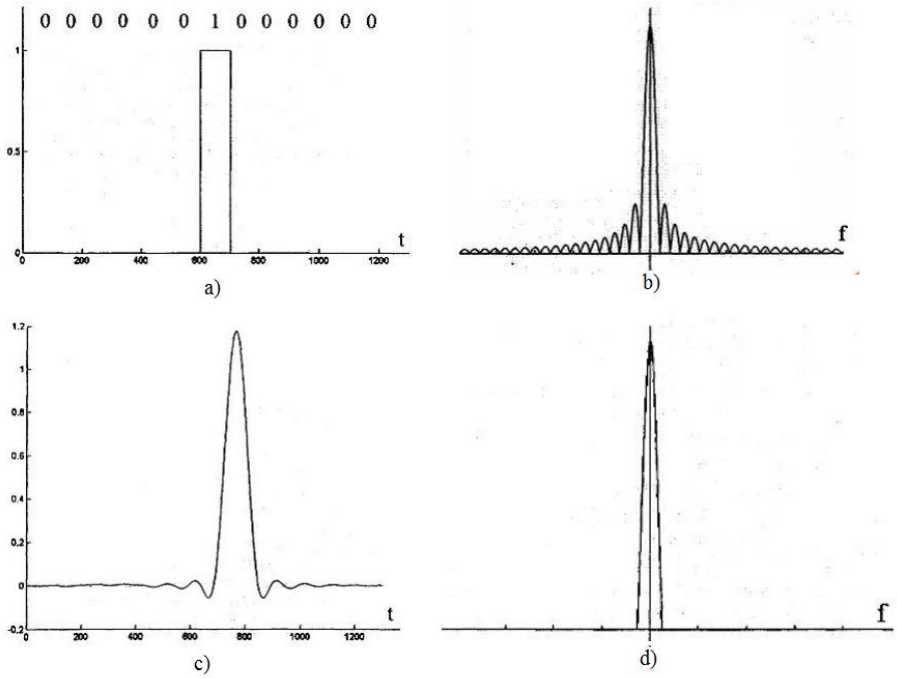

Fig 2.10. a) Signal sent in time domain by means of OOK Modulation; b) frequency components of the signal sent; c)signal received in time domain; d) frequency components of the signal received.[43]

In numeric transmission, when rectangular impulse with one byte time slot of T_b width are used, the frequency spectrum of the impulse takes shape according to $D(f) = T_b sinc(fT_b)$ function as can be seen from Figure 2.10. The frequency spectrum of the rectangular impulse in the form of $sinc\ (.)$ extends from negative infinity to positive infinity. To prevent the distortion of the impulse shape during transmission, a channel with unlimited bandwidth must be used. However, a channel in possession of infinite bandwidth does not exist. Furthermore, frequency spectrum is a very limited communication source and use of high bandwidth for communication causes inefficiency. Use of rectangular impulse in transmission may

cause a part of the frequency components desired to be transmitted due to the limitation indicated above not to reach the receiver. Distortions could occur on the impulse forms obtained at the receiver. In other words, when transmission is conducted over a channel with limited bandwidth, the communication channel limits the frequency spectrum of the signal transmitted. Limitation of the frequency spectrum of a signal would lead to the propagation of the impulse form in time-space. The impulse propagating in time goes beyond the bit time slot reserved for it to overflow into the time slots of the neighboring pulses. This circumstance gives rise to ISI problem similar to the signals received through different tracks in VLC causing differences in the receiving time of the incoming signals at the receiver.

ISI reduces the probability of correct detection of the symbols in the neighboring time slot. Therefore the transmission performance of the system decreases. The idea that first comes to mind to be able to solve the problem is to keep the bandwidth sufficiently large, in other words to keep it a few times more than $f_b = 1/T_b$that is called the symbol ratio, and to transmit the major part of the spectrum of the impulse in $sinc(.)$ form. In $sinc$ $(.)$spectrum, a major part of the energy is in the section of the spectrum extending up to $f_b = 1/T_b$frequency, thus reserving a bandwidth much larger than this frequency range would lead to the inefficient use of the communication sources.

Another solution is to change the shape of the rectangular impulse. To limit the frequency band of the impulse shape desired to be transmitted by using a low migration filter at the receiver would change the rectangular shape of the impulse and as such named as impulse shaping. The name of the filter used for this purpose is impulse shaping filter. Due to the fact that the frequency band of the transmitted

impulse is limited, the bandwidth of the signal transmitted would be reduced. As such more efficient spectrum use will be achieved. When the spectrum of the naturally transmitted signal is limited, it would not be possible to limit signal received at the receiver in the time-space. The propagation of the signal in time-space after it is limited in terms of frequency, could not be avoidable. Under the circumstances we should find an impulse with the maximum amplitude at the central point of the symbol time slot when the interference effect from the pulses in neighboring time slots is the least while having zero amplitude at the central point of other symbol time slots. When we use an impulse form defined as $d(t) = sinc(t/T_b)$ for transmission, this signal takes on zero value at the middle point of the neighboring time slots and under ideal conditions the ISI effect is not witnessed at the central point sensor. This is known as Nyquist's zero ISI criteria. When binary transmission rate is shown as R_b bit/s the bit time slot will be $T_b = 1/R_b$second. When $d(t) = sinc(t/T_b)$ type of impulse is used for transmission, the frequency spectrum of this impulse will be a rectangular spectrum that is limited to $R_b/2$. As such numeric transmission can be realized over $R_b/2$ Hz bandwidth at the rate of R_b bit/s. An analysis of the spectrum of this impulse shows it to be an ideal low migration filter spectrum. Due to the fact that an ideal low migration filter is of infinite length, it would not be possible to design one in practice. For this reason, for numeric transmission at R_b bit/s rate, $R_b/2$ Hz band width is considered to be the theoretical minimum band width. Moreover, the impulse in the form of $sinc\left(\frac{t}{T_b}\right)$is relatively slow to fade thus in case of a synchronization error that could in practice occur between the transmitter and receiver, this could cause serious amount of ISI generation. Consequently, $sinc\ (.)$ impulse could not go beyond finding a theoretical solution to the problem. For this reason, in application, Raised Cosine Filter is used

that maintains zero migration of $sinc\left(\frac{t}{T_b}\right)$ impulse but fades faster and is a limited impulse type in time. Frequency response of Raised Cosine Filter is defined by means of Eq. 2.23.

$$H(f) = \begin{cases} T_b & 0 \le |f| \le \frac{1-\beta}{2T_b} \\ T_b cos^2\left[\frac{\pi T_b}{2\beta}\left(|f| - \frac{1-\beta}{2T_b}\right)\right], & \frac{1-\beta}{2T_b} \le |f| \le \frac{1+\beta}{2T_b} \\ 0 & |f| > \frac{1+\beta}{2T_b} \end{cases} \quad (2.23)$$

β that is used in the equation, is defined as the attenuation factor and takes on values in the range of $0 \le \beta \le 1$. The attenuation factor is defined by means of Eq. 2.24 whereby, theoretical minimum bandwidth is $R_b/2$, excess bandwidth on the other hand is f_x.

$$\beta = \frac{f_x}{R_b/2} \quad (2.24)$$

Spectrum of Raised Cosine impulse for $\beta = 0$ turns into rectangular form and for $\beta = 1$ a fully raised cosine. Raised cosine filter's Frequency response and impulse response are shown in Fig.2.11.

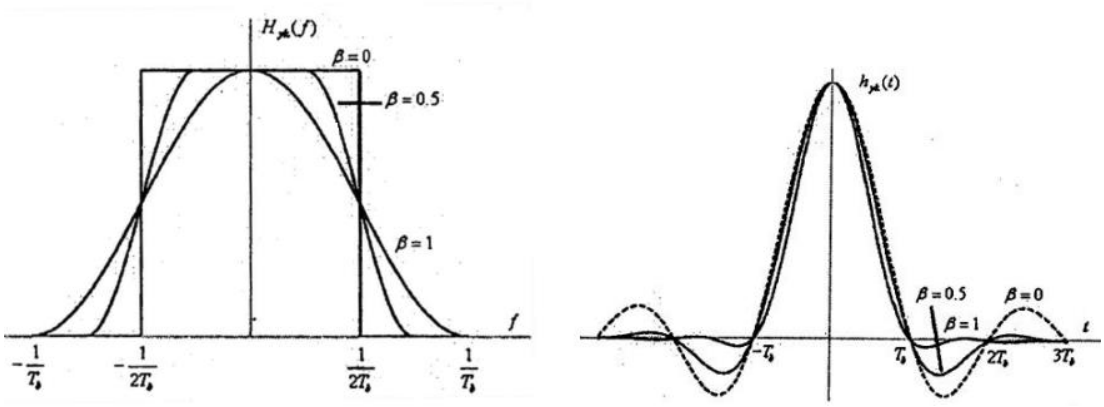

Figure 2.11 Requency response and impulse response of Raised Cosine Filter [43]

2.6.2 Adaptive Channel Equalization

The source of the major part of issues encountered in broadband communication systems is the communication channel. The inter-symbol interference caused by stringed out multi-path limited bandwidth channels leads to bit errors in the receiver. The inter-symbol interference is shown as the major obstacle facing high-speed data communication through VLC channels. The negative channel effects in the receiver, which substantially diminish the system performance, need to be resolved somehow. This process is named as Channel Equalization. The channel equalization process actually is the rerouting of the signal received in reverse through the channel. In order to achieve this, the channel information or otherwise the direct reverse has to be obtained in the receiver. To serve this purpose various algorithms are used to determine the channel equalizer. The channel and the channel equalizer are two filters connected in series. The impulse response of this new filter, which is composed by these two filters, determines as to what extent the ISI in the system may be eliminated. The channel filter and the channel equalization filter are inverse filters of each other. Since the channel equalization filter has to be of an infinite length, it is not possible to completely remove ISI. Instead of this it is aimed to regress it within the limits that will ensure communication quality.

In case the communication channel changes over time, the channel equalizer has to be able to track the variations in the channel. This type of channel equalization is named as adaptive channel equalization. The method that stands out for the use of this job in literature is the DFE. The logic behind the DFE is based on cutting off the interference of the symbols called the train set, which are previously decided upon, formed with the symbols that follow them and removal of these symbols prior to taking a decision. As observed in Fig 2.12, DFE diagram consists of two parts, namely Feedforward filter (FFF) and Feedback filter (FBF). The first one is a

feedforward filter, which is applied to the signal that comes from the channel output and is in Linear Transversal Equalizer (LTE) structure shown in its input as y_k. Whereas the second part is feedback filter applied to the symbols shown with d_k and for which decision has previously been taken with regards to its input. The function of this filter is to remove the interference the previously decided upon symbols will generate on the symbols to be decided upon.

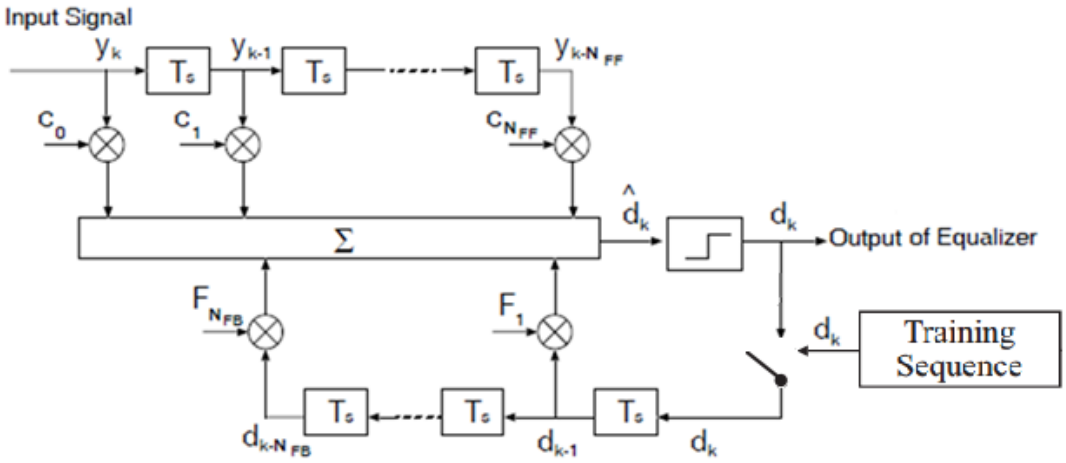

Figure 2.12 Block diagram of Decision Feedback Equalizer

The blocks that are shown in Figure 2.12, T_s show the time lag. The filter has N_{FB} number of feedback filter coefficient and $N_{FF} + 1$number of feed forward filter coefficient. The equation that shows the input output associations in the DFE filter is shown with Eq 2.25.

$$\hat{d}_k = \sum_{i=0}^{N_{FF}} y_{k-i} c_i + \sum_{i=1}^{N_{FB}} d_{k-i} F_i \qquad (2.25)$$

The DFE is being trained with a training sequence and the first coefficients are obtained with the help of this string. As the symbols solved after this first adjustment are adequately reliable, the purpose should be to move to a study with decision orientation from adaptive equalization training phase. Following this, the equalization coefficients are constantly adapted by using the error signal that is

generated as the variance between the decision taken at the detector output and the difference at the equalizer output. Since the probability of occurrence of an error at the detector output is most unlikely, the effect of such errors on the operation of the equalizer tend to be low.

The methods that adjust the DFE filter c_i and F_i coefficients of the DFE filter in a manner to minimize the filter error are called training algorithms. These methods may be addressed in two basic groups; the slope based algorithms and the least squares based algorithms [44]. The slope based algorithms have the advantage of having low process load, and are preferred in high sampling speeds and mostly in adaptive signal processing and communication applications. These are the LMS, Normalized LMS (NLMS), and Affine Projection (AP) algorithms [44]. However these algorithms have the disadvantage of slow convergence speed depending on the Eigen value propagation of the correlation matrix of the input signal. On the other hand, the least squares based algorithms are preferred due to their convergence properties being much better that slope based algorithms despite their high processing load. Recursive Least Squares (RLS) algorithm is a good example for this group. However situations that require high sampling speed limit the areas of use of these algorithms due to the intensive processing load.

As is known, the LMS algorithm is an estimated version of the gradient descent optimization method. In order to find the optimum parameters in the gradient descent method, the direction and size of the next step is determined in the calculation of the next parameter value by first starting with the initial value. The direction of the next step is determined by the derivative of the mean square error function. Eq. 2.26 may combine the feed forward and the feedback filter coefficients, which are used in the

DFE filter, within a single vector with the purpose of simplifying the presentation of the equations of the LMS method.

$$\boldsymbol{w} = \left[c_0, c_1, \dots, c_{N_{FF}}, F_1, F_2, \dots, F_{N_{FB}}\right] \tag{2.26}$$

In the same manner, the inputs of feed forward and feedback filters can also be combined as in Eq. 2.27.

$$\boldsymbol{Y}_k = \left[y_k, y_{k-1}, \dots, y_{k-N_{FF}}, d_{k-1}, d_{k-2}, \dots, d_{k-N_{FB}}\right] \tag{2.27}$$

In this case the coefficients are determined with Eq.2.28 according to LMS method in order to show the n iteration index.

$$\begin{aligned} \hat{d}_k(n) &= \boldsymbol{w}^T(\boldsymbol{n})\boldsymbol{Y}_k \\ e_k(n) &= d_k(n) - \hat{d}_k(n) \\ \boldsymbol{w}(n+1) &= \boldsymbol{w}(n) + \mu e_k(n)\boldsymbol{Y}_k \end{aligned} \tag{2.28}$$

The most important advantage of the LMS algorithm is the fact that a low number of multiplication operations are performed in the execution of the algorithm. The μ step parameter should be selected in the $0 < \mu < 2/\lambda_{max}$ range in order for the LMS algorithm forecasts to converge in a stable manner with the optimum parameter value. Here, the λ_{max} is the maximum Eigen values of the correlation matrix [45]. One of the major deficiencies of the LMS algorithm is the challenge to select a μ step parameter, which will be low enough to ensure the stability of the algorithm while being high enough to ensure convergence of the parameter forecasts to the optimum value.

The RLS is an adaptive filter which recursively finds the coefficients that minimize a weighted linear least squares cost function relating to the input signals. This is in contrast to other algorithms such as the LMS that aim to reduce the mean square error. In the derivation of the RLS, the input signals are considered deterministic, while for the LMS and similar algorithm they are considered stochastic. Compared to

most of its competitors, the RLS exhibits extremely fast convergence. However, this benefit comes at the cost of high computational complexity. The iterative equation that the RLS method applies is stated with Eq. 2.29. In these equations, the iteration index i is again shown with n.

$$\begin{aligned} \boldsymbol{S}(n) &= \boldsymbol{P}(n-1)\boldsymbol{Y}_k \\ \boldsymbol{k}(n) &= \frac{\boldsymbol{S}(n)}{\beta + \boldsymbol{Y}_k^T \boldsymbol{S}(n)} \\ \xi(n) &= d(n) - \boldsymbol{w}^T(n)\boldsymbol{Y}_k \\ \boldsymbol{w}(n) &= \boldsymbol{w}(n-1) + \boldsymbol{k}(n)\xi(n) \\ \boldsymbol{P}(n) &= \beta^{-1}\boldsymbol{P}(n-1) - \beta^{-1}\boldsymbol{k}(n)\boldsymbol{Y}_k^T\boldsymbol{P}(n-1) \end{aligned} \tag{2.29}$$

It is obvious that the method requires an initial value for the $\boldsymbol{w}$ and $\boldsymbol{P}$ variables it uses. The variable from among these values, which shows the weight should initially commence the iteration with zero $\boldsymbol{w}(0) = 0$. Whereas $\boldsymbol{P}$, which is an intermediate variable, is a matrix $\boldsymbol{P}(0) = \delta^{-1}\boldsymbol{I}$ in the manner of only diagonal element being other than zero, with all other elements being zero. The δ coefficient, which ensures the calculation of initial diagonal elements, is a constant positive coefficient that needs to be selected as low for signals that have high SNR, whereas it needs to be selected as high for signals that have low SNR. The β found in the equation is the forgetting factor and is the control parameter of the RLS method.

CHAPTER 3 IMPLEMENTATION OF SIMULATION MEDIUM

The details of the simulation medium generated within the scope of the thesis are explained in the sub sections of calculation of illumination created in the medium, calculation of the total optical force that effects the surface, calculation of the impulse response of the communication channel according to the position of a special transmitter, and calculation of the theoretical SNR and theoretical BER values.

3.1 Simulation Medium

In order to observe the effect of the medium on the communication, a house room is taken into consideration. Data is being transmitted to users through LED lamps that disseminate light that has a certain illumination area. Data that will be coming with RF broadcast is provided by optical path. Only a single path communication is being examined. There is, for instance, a photodiode in the laptop. On the other hand LEDs in groups have been simulated for the receiver. The simulated room is 2.5-meter high, and has a base area of 5x5 meters. It has been assumed that there is a transmitter on the desk with a 0.85 m height at any point of the room. Furthermore at the ceiling of the room there are 4 groups of LEDs. There are 3600 LEDs in each LED group. The LEDs are aligned in the shape of squares as 60x60 with a 1-cm gap

between each other. The representative drawing of the simulation medium is seen in Fig 3.1.

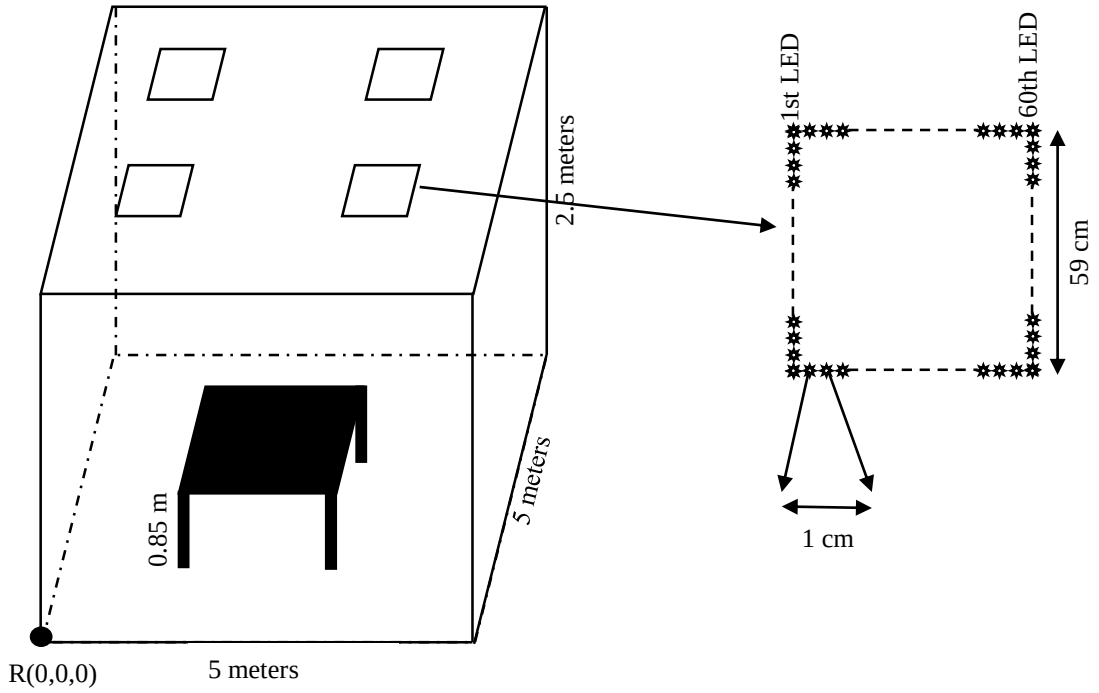

Figure 3.1 Simulation Medium

The LED groups are distributed symmetrically throughout the 5x5-meter sized ceiling. The coordinates of the R reference point of the room of the centers of the LED groups are; (1.25, 1.25, 2.5), (3.75, 1.25, 2.5), (1.25, 3.75, 2.5), (3.75, 3.75, 2.5). The specifications of the LEDs used, the specifications of the photodiodes used, and some of the medium parameters, and the symbols of these parameters used in the equations are summarized in Table 1.

In order to simulate the light that radiates from the LEDs at the ceiling of the room, the base of the room and its four walls were divided into squares with 0.2-meter side lengths, and each square was considered as the smallest unit for which simulation was performed for. The base of the room was separated into 25x25 units of grids, and

each wall into 13x25 grids. The calculations were performed for a total of 1925 grids.

Table 3.1 Simulation Parameters

Features	Values
Transmitted optical power ($\boldsymbol{P_t}$)	20 [mW]
Semi-angle at half power ($\boldsymbol{\Phi_{1/2}}$)	70 [deg.]
Center luminous intensity ($\boldsymbol{I(0)}$)	0.73 [cd]
Number of LEDs	3600 (60 × 60)
LED interval	1 [cm]
Size of LED light	59 × 59 [cm]
Reflective index values of walls ($\boldsymbol{\rho}$)	0.8
Location of specific receiver sensor	(0.1, 0.1, 0.85)
O/E convergence efficiency ($\boldsymbol{\gamma}$)	0.53
FOV at a receiver ($\boldsymbol{\Psi_c}$)	60 [deg.]
Detector physical area of a PD ($\boldsymbol{A}$)	1 [cm]
Gain of an optical filter ($\boldsymbol{T_s(\Psi)}$)	1
Reflective index ($\boldsymbol{n}$)	1.5
Simulation resolution	0.2 [m]

3.2 Calculation of Illumination

Eq 2.11 was used in order to calculate the amount of direct illumination that falls on the desk in the room. However this equation is only valid in instances when only one illumination source is available. As can also be seen in Fig 3.2, in a circumstance

when different illumination sources are in question, this is converted into a situation where multiple illumination sources are available, as in Eq.3.1.

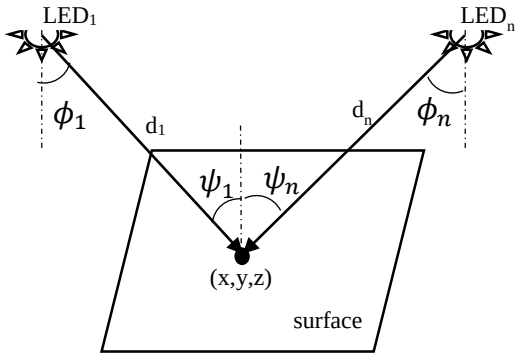

Fig 3.2 Rays that originate from multiple sources and directly reach the surface

$$E_0 = \sum_{i=1}^{n_s} I(0)cos^m(\phi_i)cos(\psi_i)/{d_i}^2 \quad (3.1)$$

The n_s expression found in the equation shows the total LED number available. It has been assumed in the equation that all light sources are the same and that they have the same center luminous intensity ($I(0)$) value. Calculation has been made for 14400 rays that fall on the 625 (25x25) grids, which form the base surface in order to calculate the direct illumination that falls on the desk. In this case, 9000000 processes have been performed for the direct illumination on the desk. Whereas for the direct illumination, which falls on the 4 walls a calculation has been made for 14400 rays that fall on 1300 (4x13x25) grids. This in turn means 18720000 processes. Whereas in total 27720000 processes have been performed for the direct illumination that falls on the entire surface.

According to Eq 3.1, the illumination amount that falls on the desk is calculated as in Fig. 3.3. The illumination amounts that directly fall on the walls have been used for the calculation of the total illumination amount by also taking into account the 1st order reflections. This is due to the fact that the light sources that can generate 1st

order reflection on the desk are the four walls of the room. The 1300 grids that represent the walls of the room, reflects the light coming from each light source to each point on the desk by behaving as a light source. Thus, in order to calculate the 1st order reflections 11700000000 (4x3600x1300x625) processes have been performed. The process executed consists of separately calculating for all the LEDs the equation given in Eq. 2.11. Under such a circumstance, the total illumination amount formed on the desk is as shown in Fig 3.4.

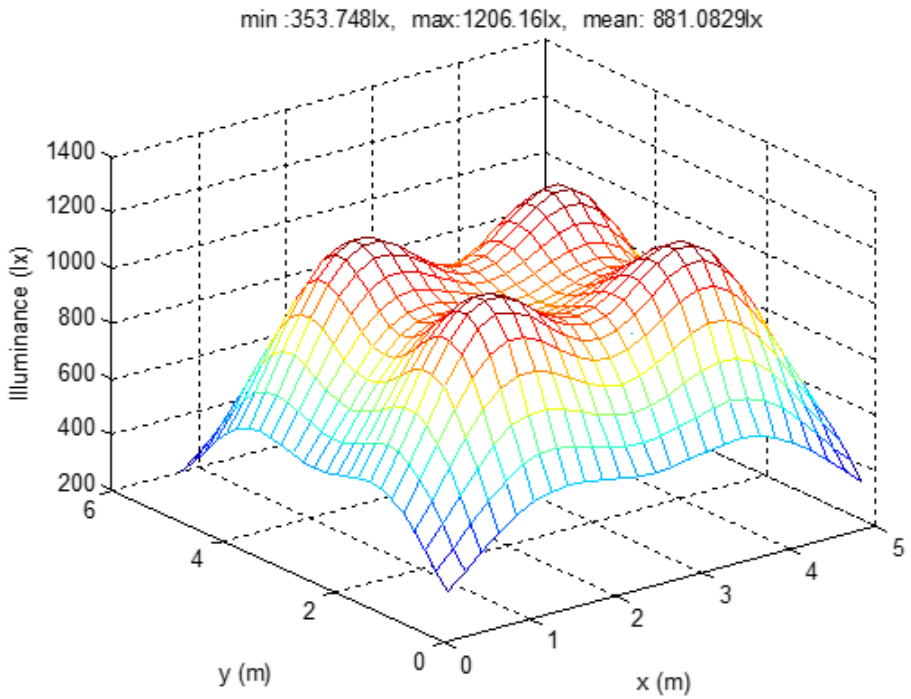

Figure 3.3 Direct Illumination on desk

According to Fig 3.4, the section of the room that is least illuminated is being illuminated by 589.93 lx, whereas the most illuminated section is being illuminated by 1023.48 lx. According to the standard stipulated by the International Organization for Standardization (ISO), the illumination amount in the office medium has to be between 300 lx and 1500 lx. Thus our simulation medium satisfies this standard.

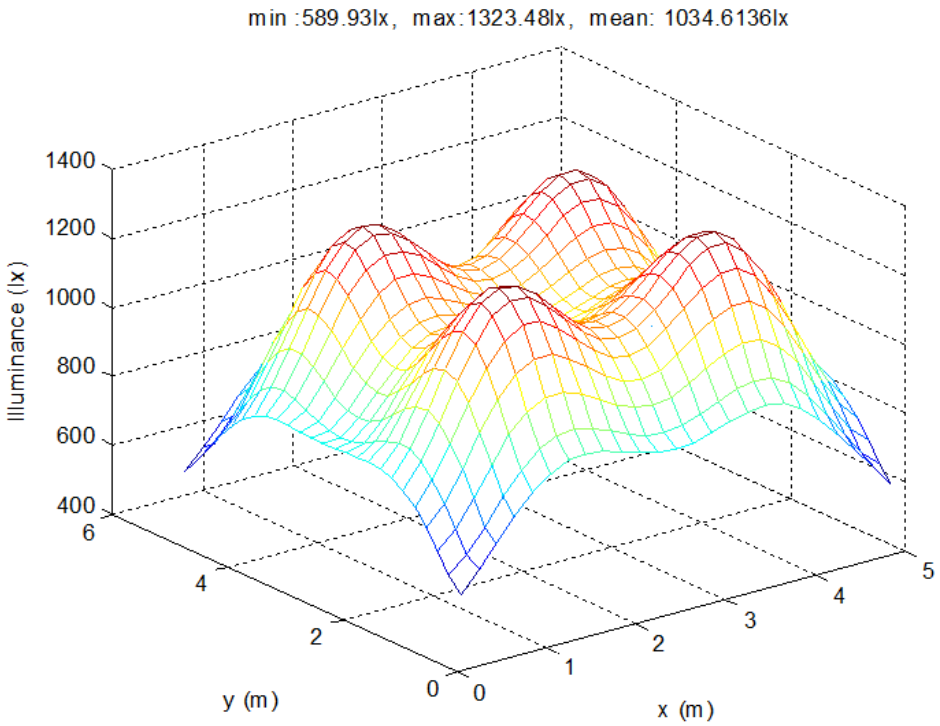

Figure 3.4 Direct and 1st order reflection's iIllumination on desk

3.3 Calculation of Received Power

The H_0 value will be used, whose equation is given in Eq. 2.14 in order to calculate the power that will fall to a given photodiode in Table 1. However the equations provided in Chapter 2 were for a single light source. The Eq. 3.2 was used to calculate the direct power the receiver that is located at any point may receive.

$$P_d = \sum_{i=1}^{n_{LED}} P_t H_{0,i} \tag{3.2}$$

The $H_{0,i}$ value found in the equation has been calculated by showing the d value, which shows the distance between the light source and the receiver in the equation given in Eq. 2.13 as d_i. In this case the direct power that falls to any position that the receiver may be located is shown by Fig 3.5.

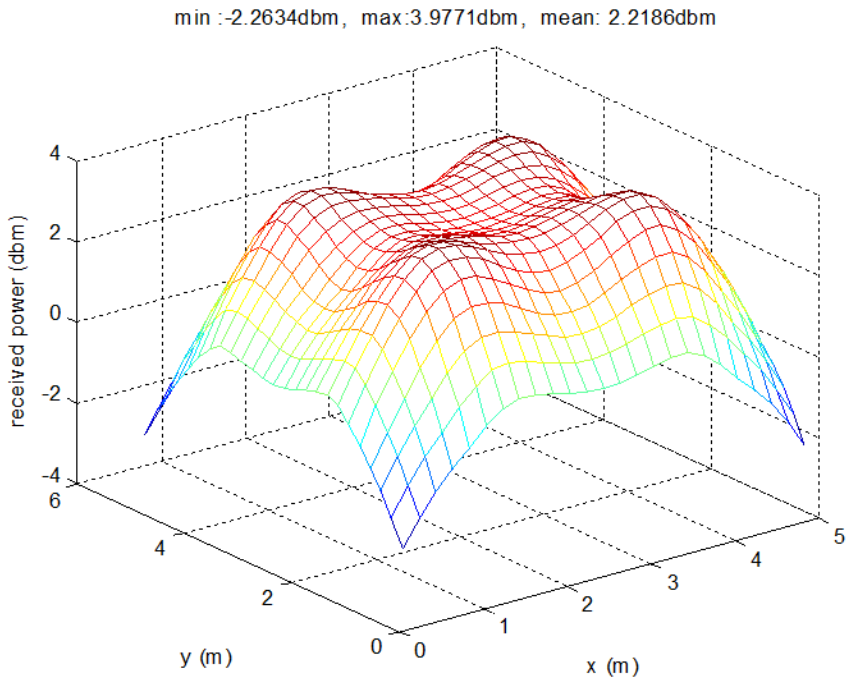

Figure 3.5 Received Power with direct illumination

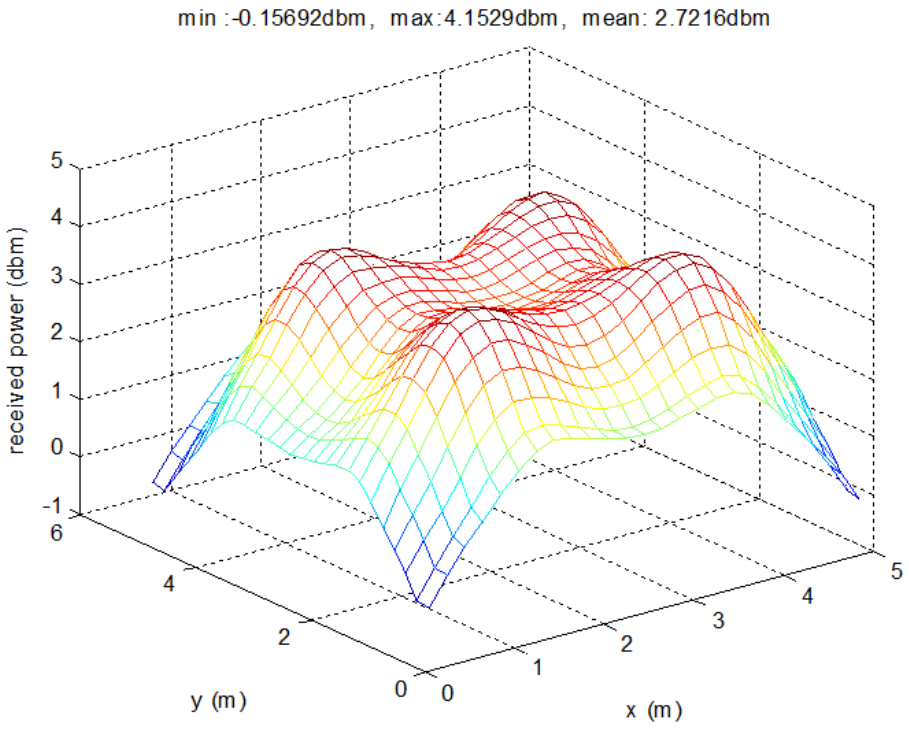

Figure 3.6 Received Power with direct and 1st order illumination

The Eq. 3.3 has been used, which is the generalized form of Eq. 2.17 under the circumstance where there is multiple light sources, in order to calculate the power the receiver detects by also taking into account the 1st order reflections.

$$P_r = \sum_{i=1}^{n_{LED}} P^i{}_{r,0} + P^i{}_{r,1} \quad (3.3)$$

The $P^i{}_{r,0}$ symbol found in this equation shows the power the direct ray originating from i LED forms at the receiver, whereas the $P^i{}_{r,1}$ symbol shows the power entire rays originating from i LED and that come by being reflected. The direct rays in the receiver and the power formed at the receiver coming from 1st order reflection are shown in Fig. 3.6. According to the results, the power formed at the receiver that is on the desk by also taking into account the 1st order reflection is on average greater than 0.51 dbm.

3.4 Calculation of Impulse Response

Entire rays coming directly from all the LEDs and through 1st order reflection to the special point where the receiver is located should be tracked in order to calculate the Impulse Response. The period of time it takes for these rays to arrive at the point where the receiver is and the power generated at the receiver should be determined. Since there are 14400 different light sources, if it is assumed that there are not any obstructions that may cause shading, a total of 14400 direct rays fall on any point. There were a total of 1300 grids on the four walls that could reflect on the desk. All these light sources will reach to these 1300 grids and will travel to the receiver from these. Thus 18720000 (1300x14400) rays shall reach the receiver by way of reflection. In this case the process in Eq. 2.19 has been performed for 18734400 rays in order to calculate the impulse response of each receiver. The impulse response of

the system with a photodiode that has a 60-degree FOV angle at (0.1 0.1 0.85) coordinate is shown in Fig 3.7.

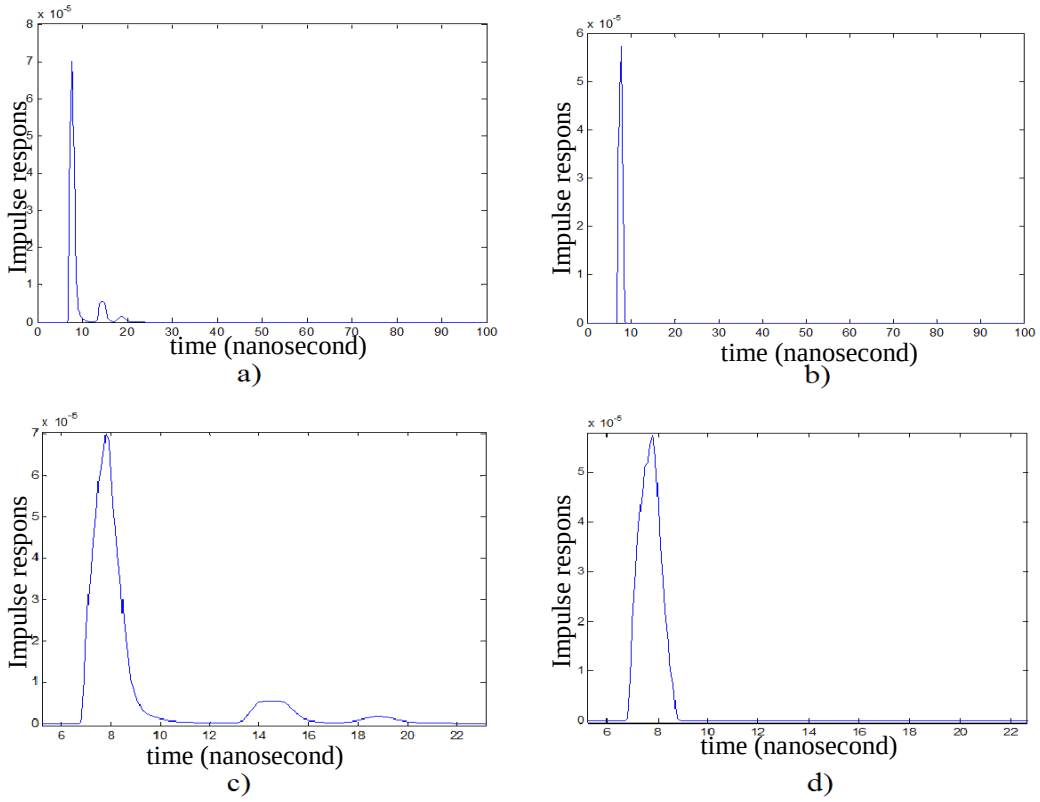

Figure 3.7 Impulse response at (0.1 0.1 0.85) for 60 deg FOV a) with 1st reflection b)only direct illumination c) with 1st reflection in time range [6 22] c) only direct illumination in time range [6 22]

As can be seen in the diagram, the maximum impulse has formed at about 8 ns. However this impulse is not a complete impulse and it can be observed that it is extended over time. Moreover another impulse is seen that is extended in time that is smaller than the main impulse and is 7 ns further away from the main impulse. The extension of the main impulse in time and the formation of other impulses in the impulse response occur due to the signal going through different paths and reaching the receiver. The shape of the signal received after the impulse responses obtained being applied to a sample input signal is as shown in Fig 3.8.

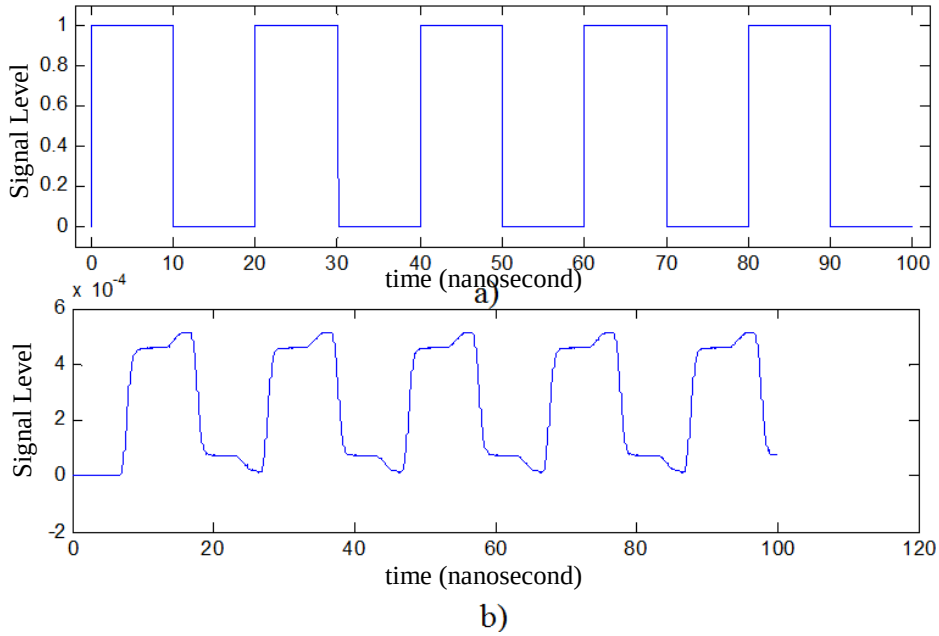

Figure 3.8 a) Transmitted Signal Level $X(t)$ b)Received signal Level $Y(t)$ at $N(t) = 0$

3.5 Mean Delay and RMS Delay Spread of Simulated Room

In the previous section it was calculated that process had to be performed for a total of 18734400 rays in order to calculate the impulse response for any one point. But as the desk may be located at any point within the room, and as the receiver may be at any point on the desk, it is necessary to calculate the impulse response for the entire base area. When it is considered that the base of the room consists of 625 grids, the total number of processes that are required to be performed reaches 11709000000.

After the impulse response is calculated for each point, the mean delay and RMS delay spread values of all base points are calculated with Eq. 2.20 and Eq. 2.21, and Fig. 3.9 and Fig 3.10 were obtained. The points where mean delay value is lowest are the points where LED centers can send rays through the shortest path, whereas the

points where the mean delay value is the highest are the points that are far away from the LED centers.

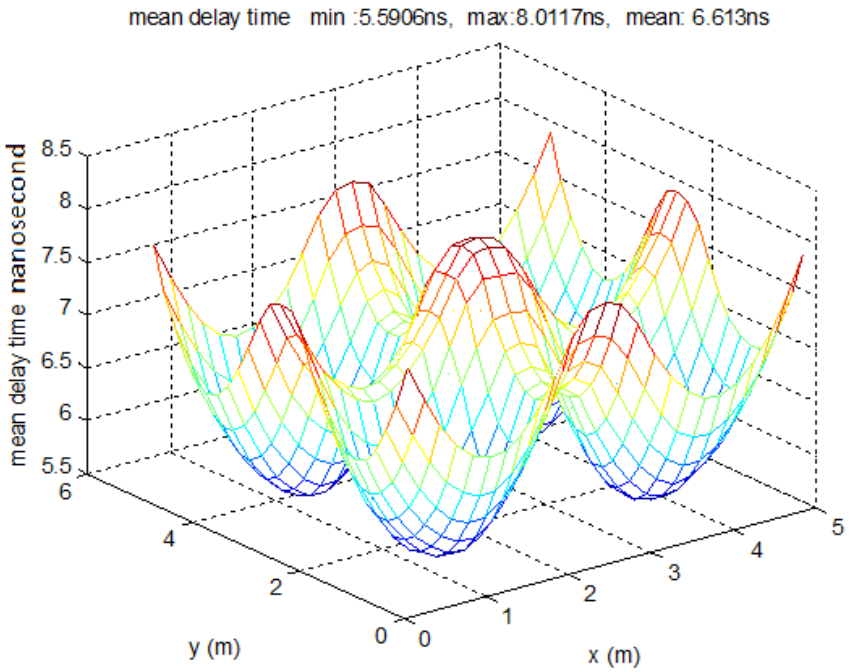

Figure 3.9 Mean Delay time at any location at desk

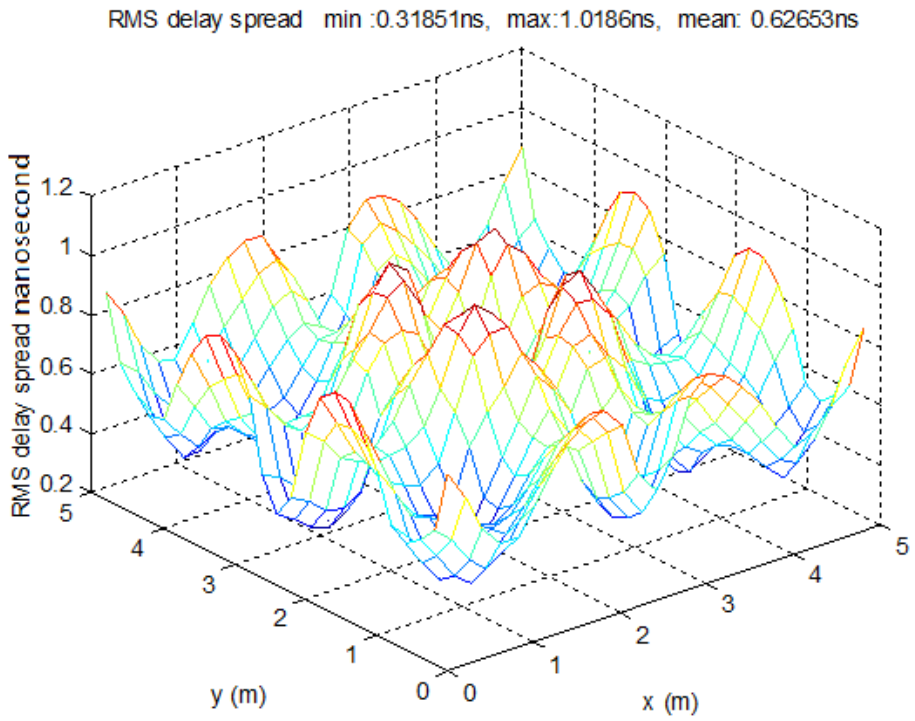

Figure 3.10 RMS Delay Spread at any location at desk

3.6 Theorical SNR and Theorical Bit Error Rate

The signal that is generated in the range of [0 T_b] impulse response with $T_b$being the symbol duration of the actual signal, and the signal between [T_b ∞] is evaluated as noise [10]. In this case, the desired received signal is written with Eq. 3.4, and received signal by ISI is written in Eq. 3.5.

$$P_{rSignal} = \int_0^{T_b} (h(t) \otimes X(t))\, dt \tag{3.4}$$

$$P_{rISI} = \int_{T_b}^{\infty} (h(t) \otimes X(t))\, dt \tag{3.5}$$

The desired signal required to be obtained from the receiver under the circumstances can be written as $S = \gamma^2 P_{rSignal}^2$ and the noise contained in the signal as $N = \sigma_{shot}^2 + \sigma_{thermal}^2 + \gamma^2 P_{rISI}^2$. If it is accepted that there is constant shot and thermal noise in all signals, the SNR ratio will be calculated for all possible points where the receiver may be placed. The SNR ratios that will form on the desk surface as $T_b = 10\ ns$ without taking into account the 1st order reflections is shown in Fig 3.11, whereas SNRs that are formed after taking into account the 1st order reflections are shown in Fig 3.12.

While the mean SNR value created on the desk is 18.8 db when only direct lighting is taken into account, the mean SNR value regresses to 15.5 when the 1st order reflection is also taken into account. These results are obtained under $T_b = 10ns$, which means that communication speed is 100Mb/sec. According to simulation, we obtained minimum 15.52 db, so it is enough for a stable communication link.

There is the $BER = Q\left(\sqrt{SNR}\right)$ relationship between SNR and the Bit Error Rate (BER) in OOK modulation [10]. The $Q(x)$ function found in the expression is shown with Eq 3.6.

$$Q(x) = \frac{1}{\sqrt{2\pi}} \int_x^{\infty} e^{-y^2/2} dy \tag{3.6}$$

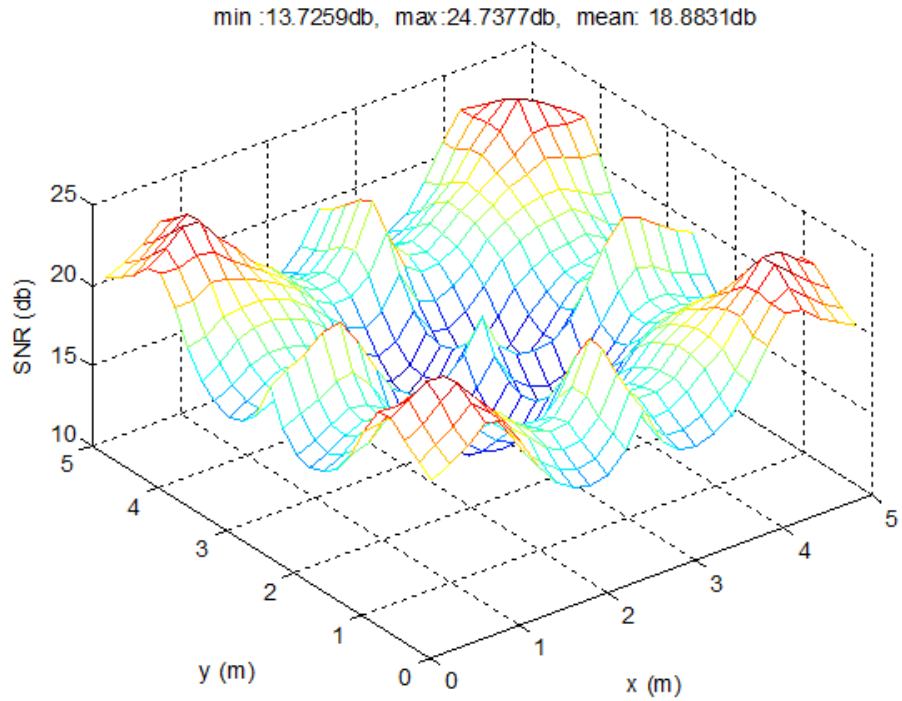

Figure 3.11 Theorical SNR under direct illumination

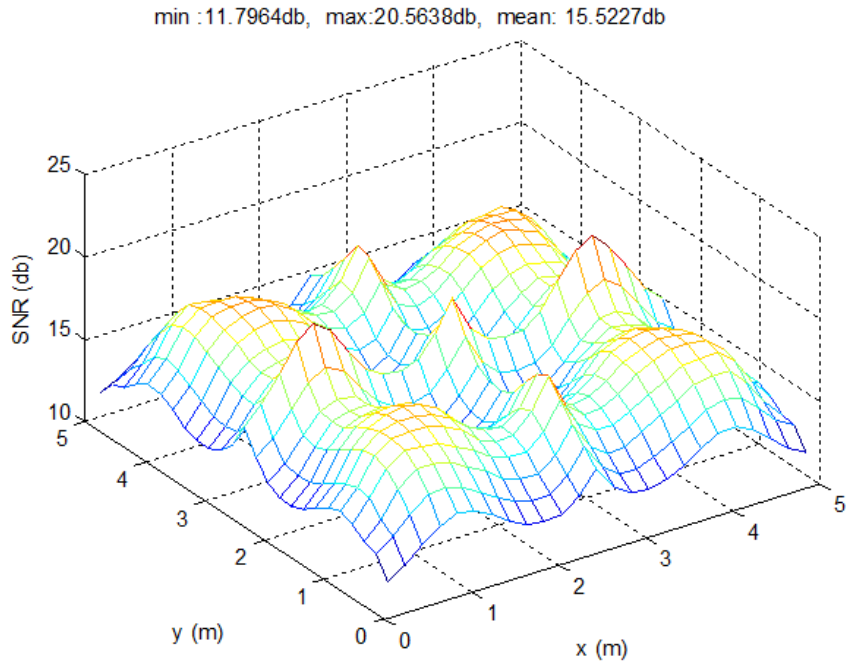

Figure 3.12 Theorical SNR under direct and 1st order reflection illumination

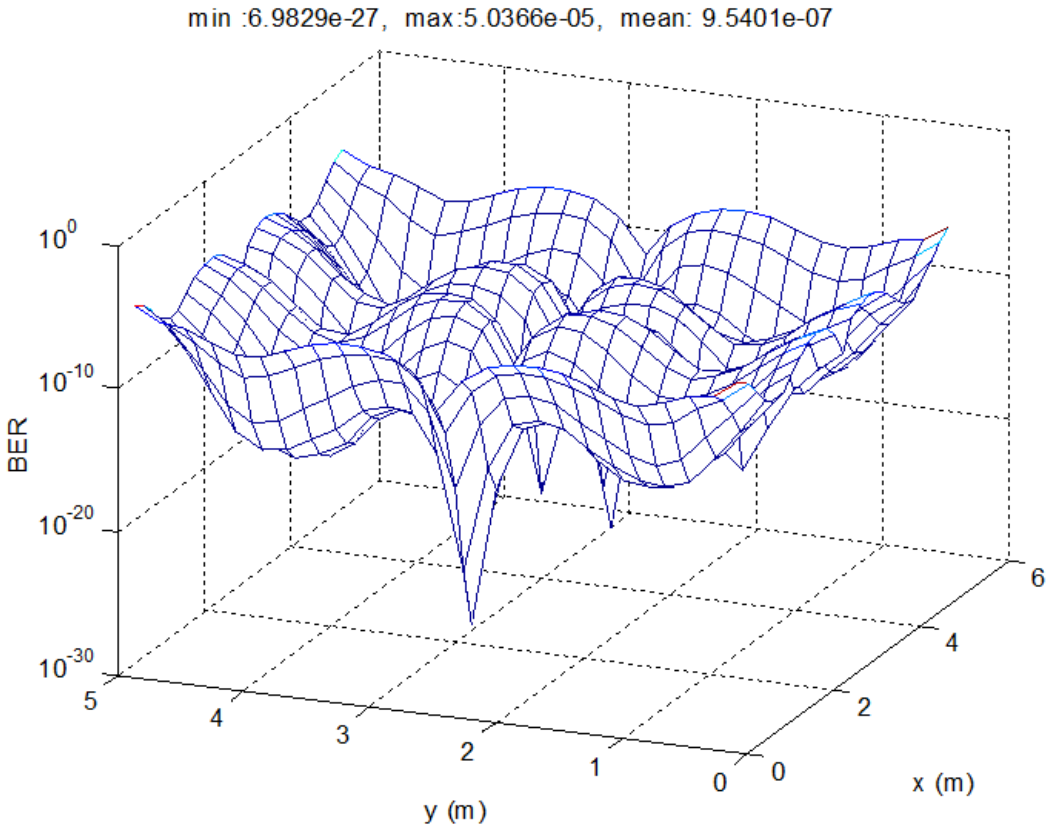

Figure 3.13 Theorical BER

In this case, the theoretical BER calculated for all the surface of the desk that is located in the simulation room is shown by Fig.3.13. The BER ratio has been calculated at the 10^{-5} level at worst, and at the 10^{-27} level at best

3.7 Implementation of Raised Cosine Filter

We implement raised cosine function with %100 excess bandwidth. This means that the roll-off factor equals to 1. The raised cosine filter frequency response is given in Fig 3.14, which is applied when $T_b = 10\ ns$. Whereas the signal generated upon the signal passing through the Raised Cosine Filter that is put into convolution with impulse response is shown in Fig 3.15.

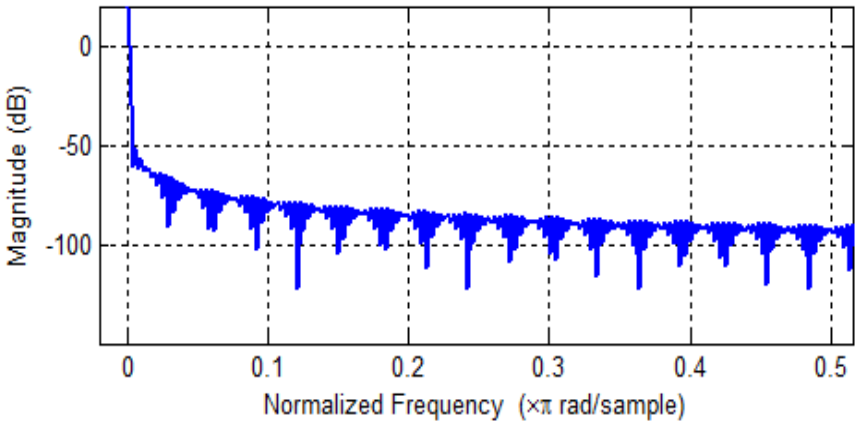

Figure 3.14 Frequency response of Raised Cosine Filter

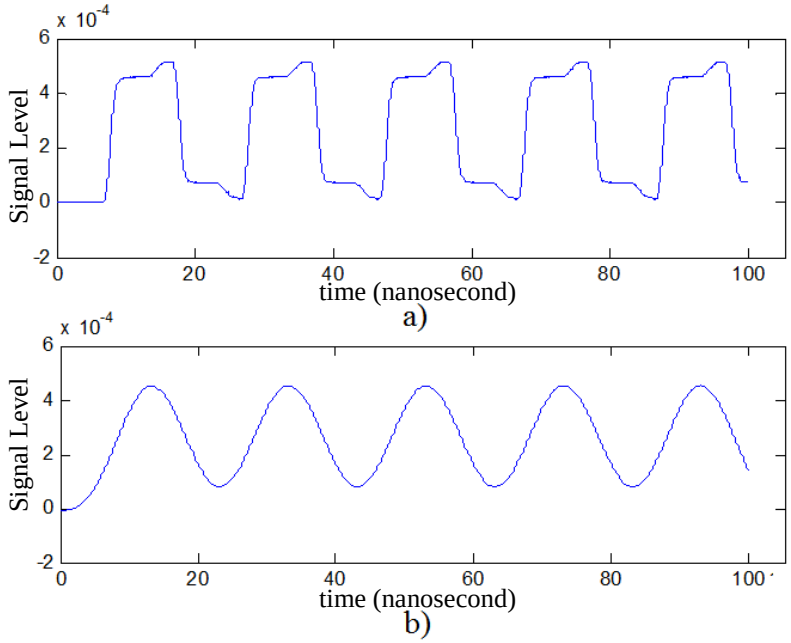

Figure 3.15 a) Received Signal before Raised Cosine Filter b) Received Signal after Raised Cosine Filter

CHAPTER 4 TESTS AND RESULTS

The VLC system will have been tested and the success of the DFE system will have been measured for the different conditions that the impulse responses will be obtained for in conclusion to the simulation. The steps of the test mechanism respectively in this section will consist of the effect of FOV, effect of symbol duration, effect of noise, effect of training noise and results of BER versus SNR at different symbol periods, and FOV sub headings.

4.1 Steps of Tests

The test mechanism, whose block diagram is given in Fig. 4.1, consists of two different pipelines, each with 5 different steps from the other. These two pipelines express whether adaptive equalization is to be used or not. At first a message is generated that consists of 100000 random symbols in both pipelines. The message that is generated is coded by using certain symbol duration according to the OOK modulation either as 1 or 0, that is to say LED being either on or off. The message signal generated with the impulse response obtained from the simulation step generates the signal that the receiver determines after passing through convolution and is multiplied by the convergence efficiency coefficient and by adding the noise that ensures the desired SNR, as shown in Eq. 2.18. Afterwards this signal is sent through the raised cosine filter that is set according to the symbol duration and excess rate value.

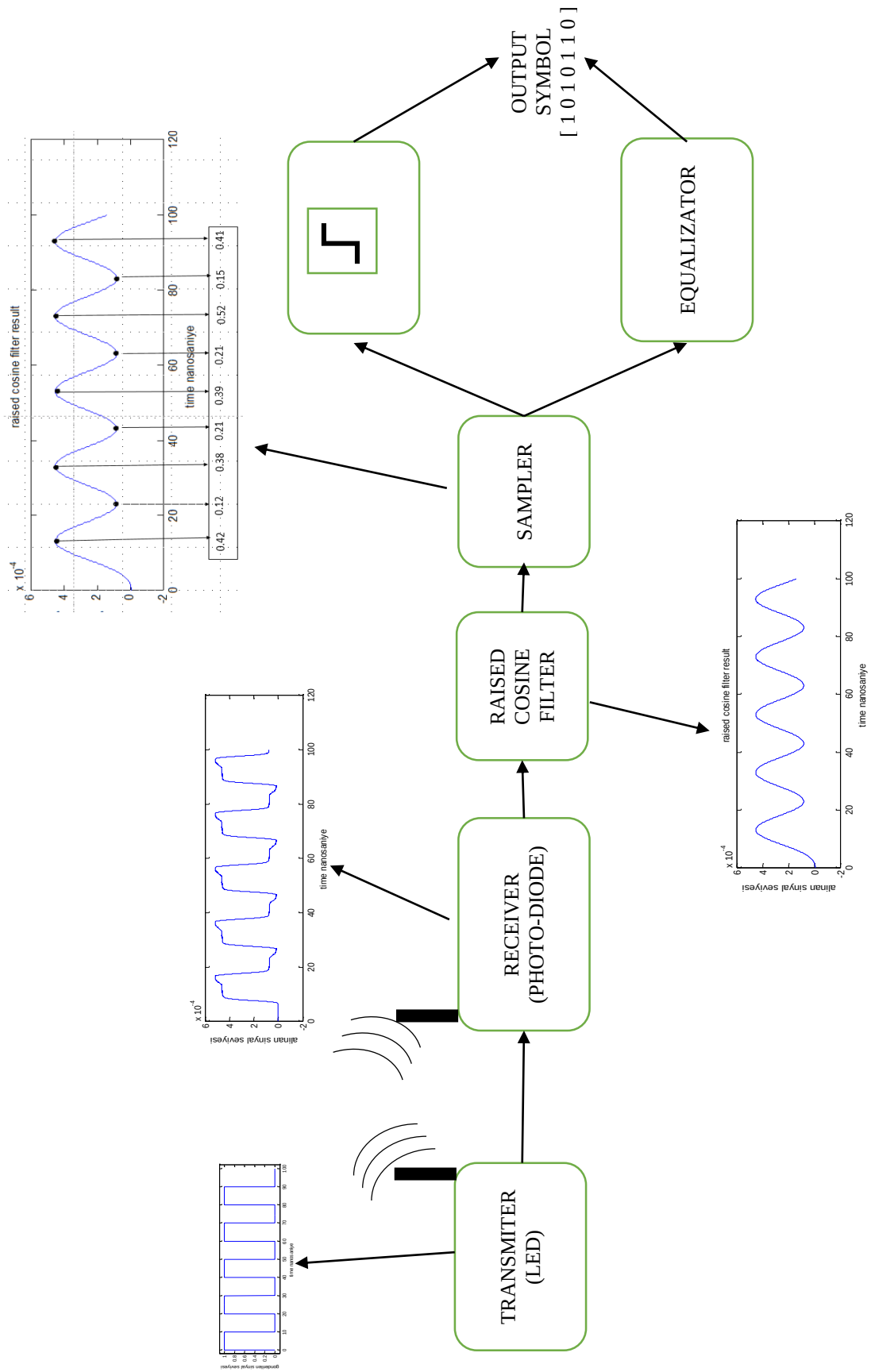

Figure 4.1 System Block Diagram

The signal is sampled in the sampler phase, as is shown in Fig 4.2 in the signal filtered with Center Point Detector by taking samples from the exact midpoint of the sample time. There are now two different tests for the signal that has been sampled. In the first one, a symbol is obtained with only a simple comparison process without passing through any equalization process. An error rate of the system is calculated by comparing the symbols actually sent and the symbol obtained.

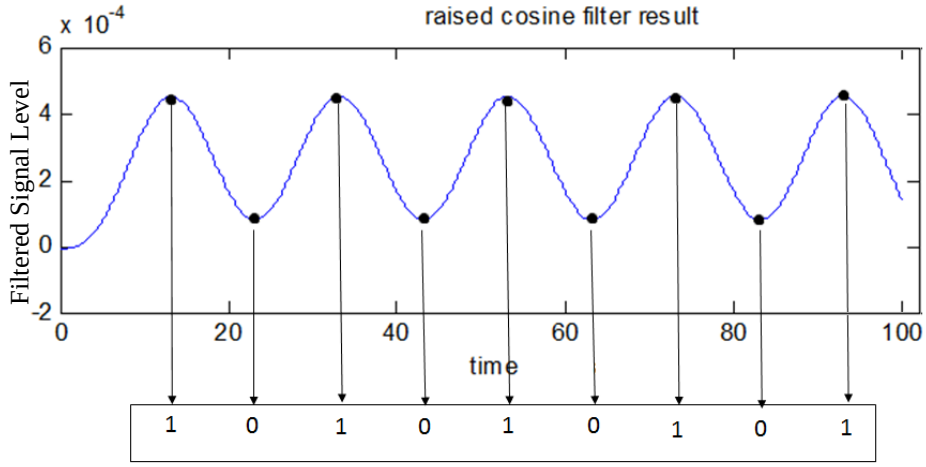

Figure 4.2 Obtained symbol by wıthout equalization

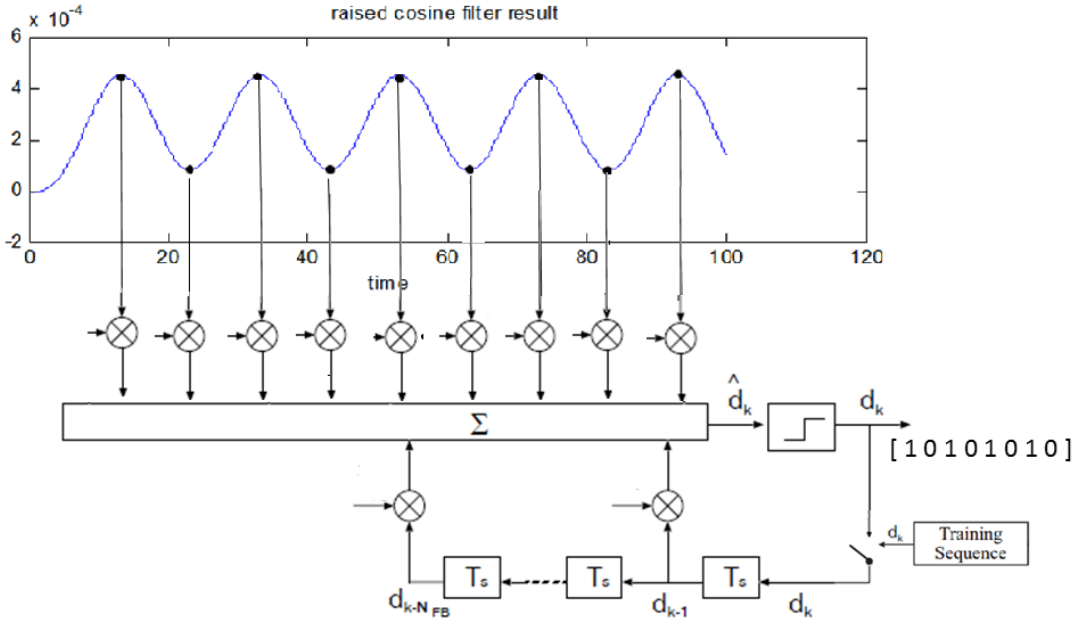

Figure 4.3 Obtained symbol by with equalization

When adaptive equalization is used, the diagram that describes the flow of the system will be like that in Fig. 4.3. The signals sent through the raised cosine filter are fed into the adaptive filter after they are sampled with the center point detector. The Adaptive filter adjusts the weights by calculating the error according to the train sequence elements throughout the train sequence period where it knows the signal that has come previously. Furthermore it constantly updates the weights by using the converted state (0, 1 status) of the symbol from the filter output following the termination of the train sequence.

4.2 Effect of FOV

The impulse responses are separately calculated by taking into consideration the fact that the receiver, whose position is assumed to be at the point with (0.1, 0.1, 0.85) coordinate, respectively has 30 deg, 60 deg and 90 deg FOV angles. The results obtained are as shown in Fig 4.4.

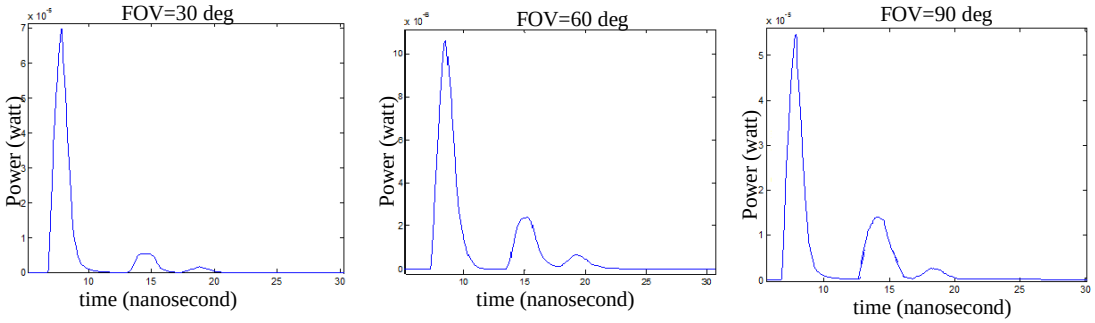

Figure 4.4 Effect of FOV

As rays that are reflected from wide FOV angles affect the receiver more, the secondary peak points ahead of the base peak point tend to be stronger. Moreover in

the FOV acute angles, rays that are at closer angles to normal receiver enter the receiver. These rays mostly consist of rays that come in directly.

4.3 Effect of Symbol Duration

Symbol duration determines the communication speed. Lower symbol duration should to be used for faster communication. However as the symbol duration is more constricted, the ISI effect starts to increase. A sample message has been generated and different symbol durations have been coded in order to show the effect of this event.

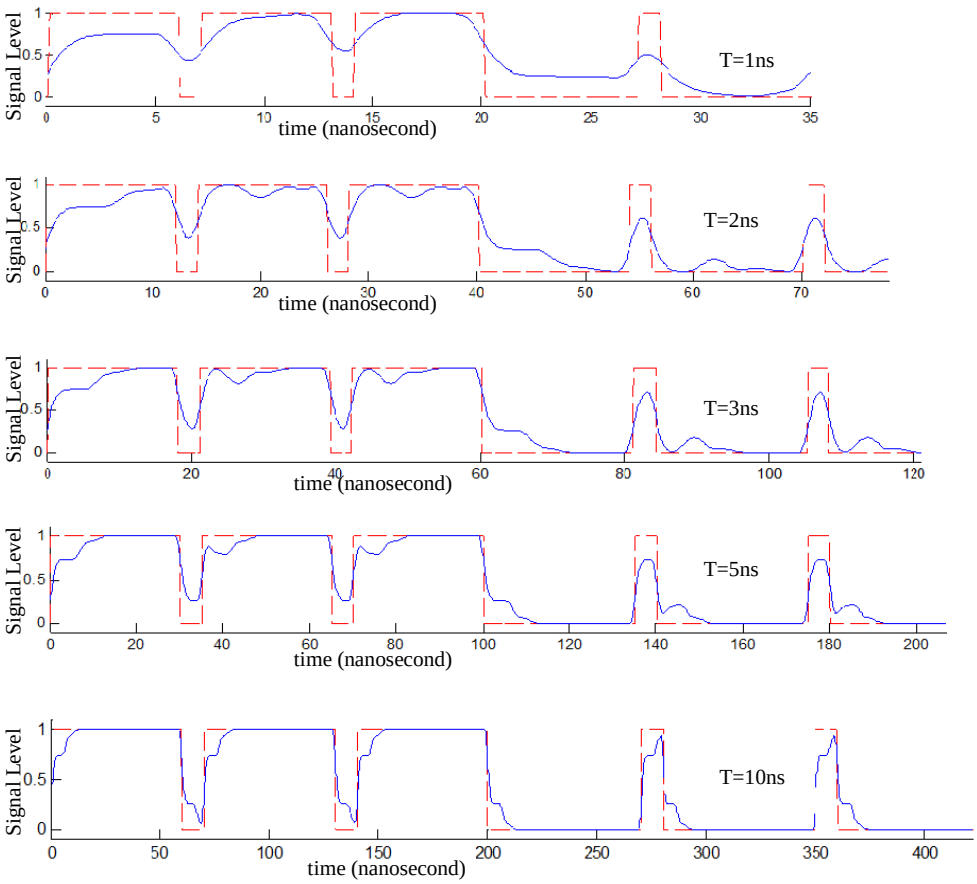

Figure 4.5 Effect of Symbol Duration

The normalized powers of the signal detected from the photodiode when 5 different symbol durations are used (T= 1 ns, 2ns, 3ns, 5ns, and 10 ns) are shown in Fig. 4.5. On the other hand, the red dashed lines seen in the diagram express the signal sent. According to the results; as ISI effect increases in communication with short symbol durations, the ISI effect decreases in communication with high symbol durations.

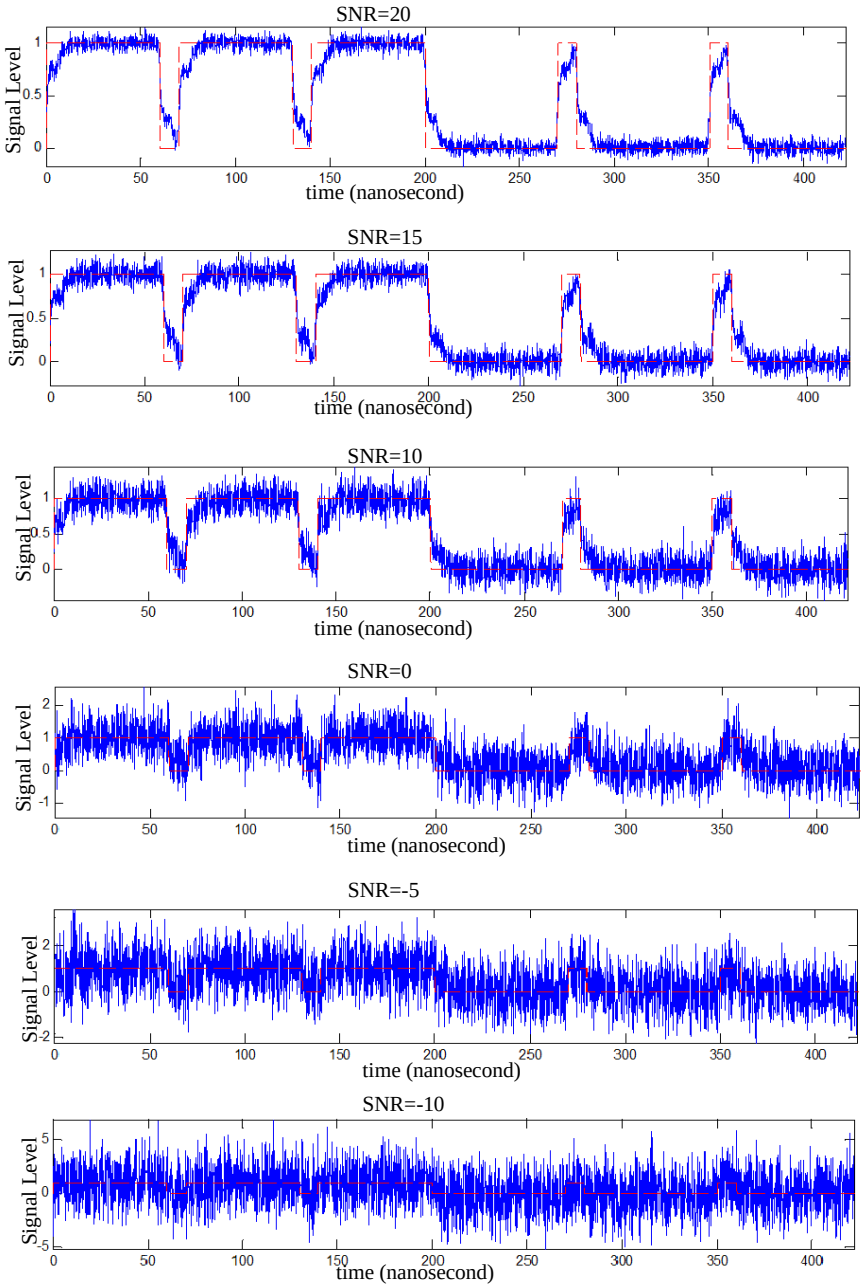

Figure 4.6 Effect of SNR

4.4 Effect of Noise

The noise parameters that affected the signal sent were explained in Section 2.5.2. When simulating the noise in the test, shot and thermal noise have not been separately modeled. The white Gaussian noise that will ensure the SNR has been added to the signal. In Fig 4.6 the signal received is seen when white Gaussian noise is added to the signal generated in a manner to form differing SNR values between -10 and +20. Sample signals have been charted for the T=10 ns symbol period. The signal sent shown with the red dashed line in the diagram expresses the signal sent.

4.5 Effect of LMS and RLS Parameters

The control parameter of LMS is the μ coefficient. This coefficient was tested empirically for different values and 0.005 was determined as the optimum value. A test was performed for T=3 ns, SNR= 0db, and FOV=60. According to Fig 4.7, LMS algorithm requires a train sequence of approximately 100 nanoseconds even at the optimum μ value.

The control parameter of RLS is the forgetting factor (β). This coefficient was empirically tested for different values and 1 was determined as the optimum value. According to Fig 4.8, it is observed that the RLS converges much faster compared to LMS. Convergence is achieved in approximately 20 nanoseconds. The test was performed for T=3 ns, SNR= 0db, and FOV=60.

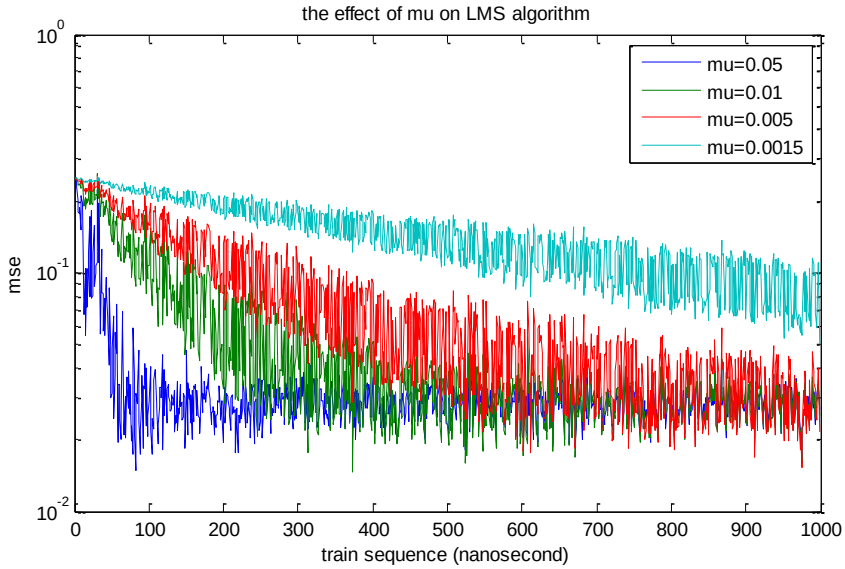

Figure 4.7 Eefect of control parameter on LMS algorithm

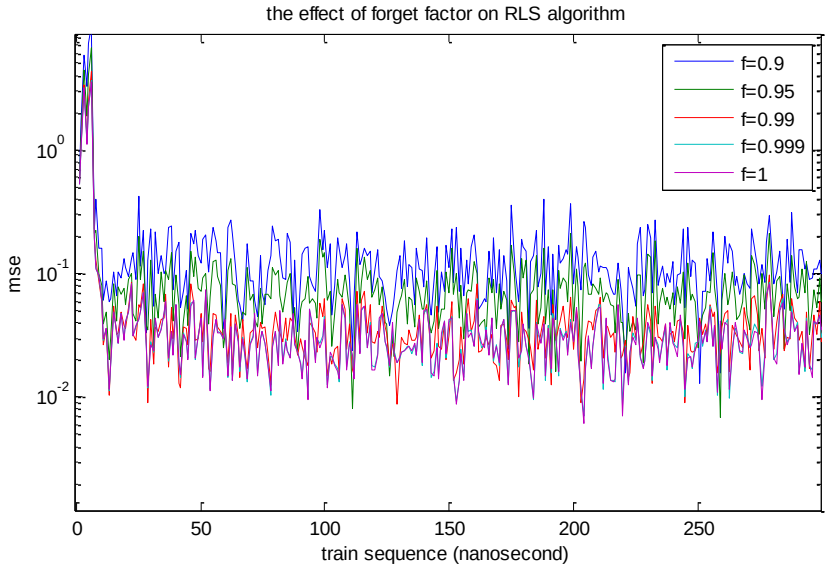

Figure 4.8 Effect of control parameter on RLS algorithm

4.6 Effect of Train Sequence Length

In order to research the effect of train sequence to performance, the train sequence was changed in the constant test mechanism. Randomly generated 10000 symbols were simulated with T=3 ns being the symbol period, FOV=60, and SNR=0 db. As

can be seen in Fig 4.9, while RLS could achieve faster adaptation and diminish the error, LMS can only adapt later.

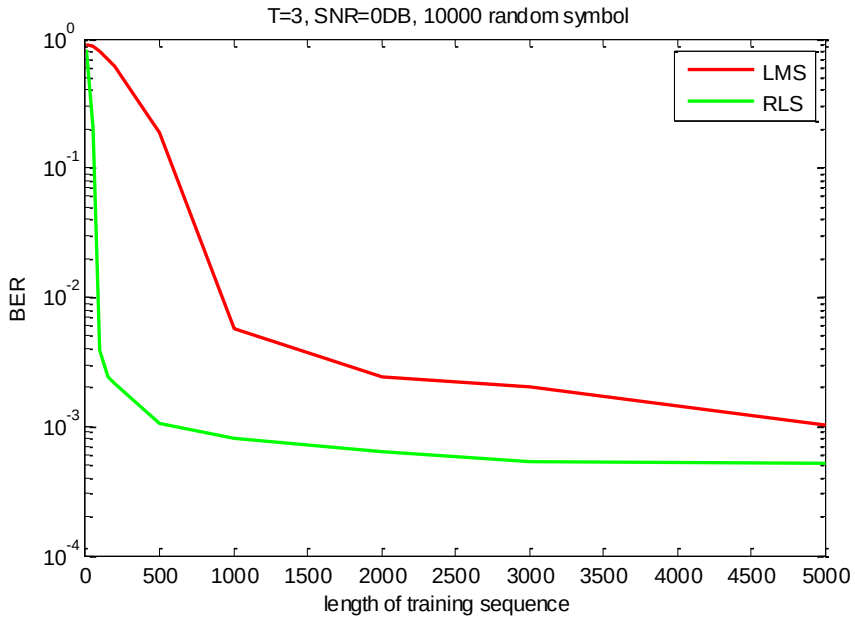

Figure 4.9 Effect of Train Sequence Length

4.7 Results of BER versus SNR, under Different Symbol Periods and FOV

The 30, 60, and 90 FOV values of the receiver were simulated separately. The T=1.9, 1.7, 1.5, and 1.3 nanosecond values were simulated separately as symbol period. Noise was added in a manner that would ensure the SNR to be 0 and +5 at 0.5 intervals. All these cases were simulated for 100000 symbols that were randomly generated. The first 10000 of the 100000 samples were determined as the train set for equalizer. The generated signals were separately filtered with LMS and with RLS without any equalizer. Comparison was made and BER values were calculated for the 90000 symbols determined as the last test cluster.

The test results are as displayed in Fig 4.10. The results in this Figure are respectively for FOV angles with 30, 60, and 90 degrees; whereas each row is the

results of tests performed for symbol durations that respectively have 1.9, 1.7, 1.5, and 1.3 ns lengths. The graphic has been formed by finding the BER value encountered after the signal is analyzed at the receiver upon signal with noise that has different SNR values have been generated. As can be seen in the graphic, in entire tests where equalizer has been used, even if the signal has noise, a lower BER ratio is reached. Concurrently, RLS is giving a lower BER ratio virtually at all times with regards to LMS.

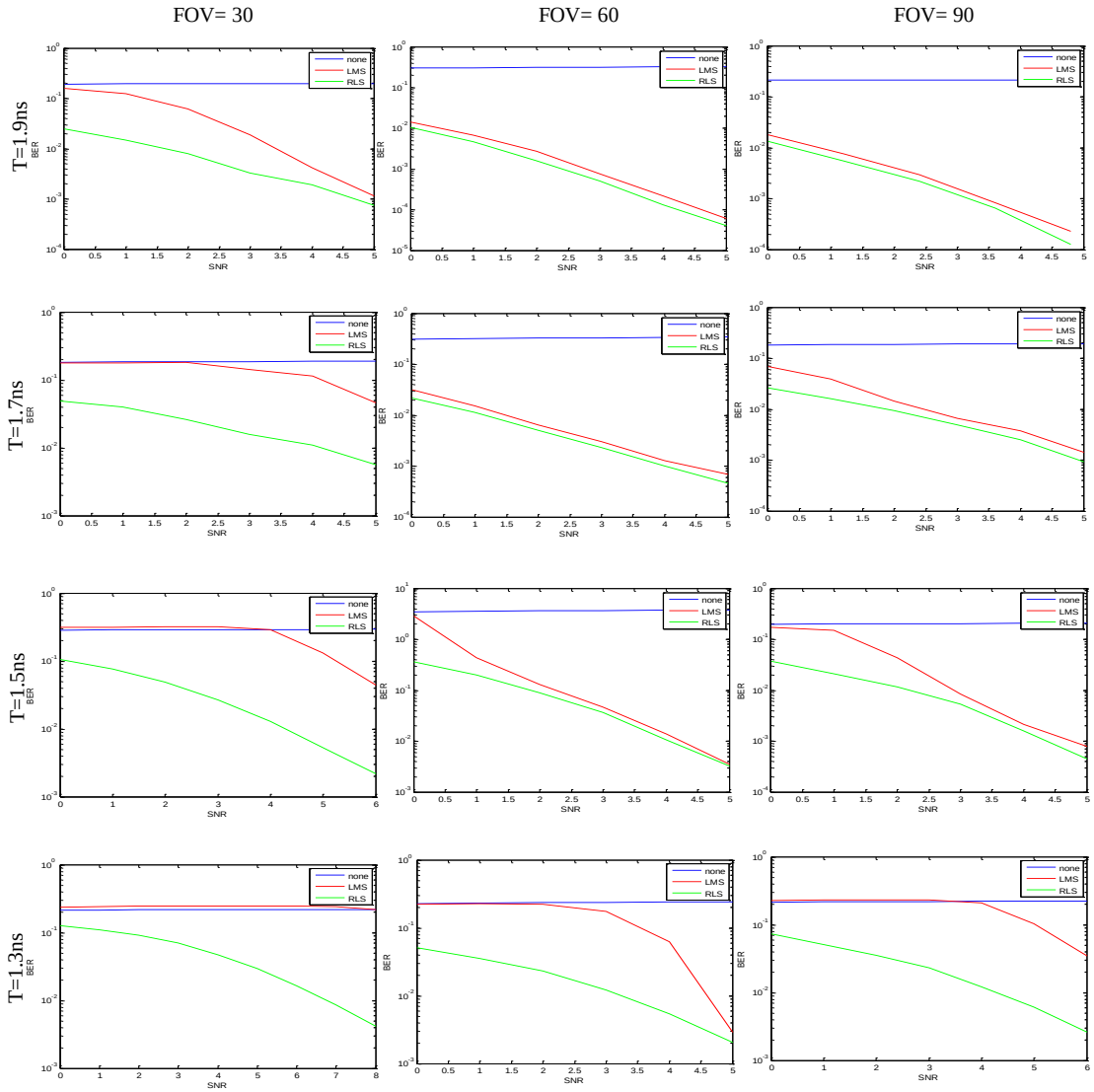

Figure 4.10 Results of BER versus SNR, under Different Symbol Periods and FOV

4.8 Comparison of Time Complexity of LMS and RLS

The recursive least squares (RLS) algorithm has generally faster convergence than least mean squares (LMS). Our results in Section 4.5 and 4.6 is supported this knowledge as well. According to iterative process of LMS in Eq. (2.28) and iterative process of RLS in Eq. (2.29), it is obvious that RLS algorithm need much more calculations than LMS. LMS has only $\boldsymbol{O(n)}$ complexity according to number of DFE tab's. On the other hand, RLS has $\boldsymbol{O(n^2)}$ complexity according to number of DFE tab's [46]. But in all test we did not tested time consumption under different tabs number. We used the same number of tabs such as 10 tabs for feed forward coefficients, 5 tabs for feedback coefficients. In this section we only tested time consumption of RLS and LMS under different signal length. According to Eq.2.28 and 2.29, all two algorithm have linear time complexity under signal length. But RLS has more calculations. The time consumption of RLS and LMS under different signal lengths is shown Table.4.1. Programs run on i7 based 2.4 GHz, 8 GB Ram PC with Matlab 2014a.

Table 4.2 The time consumption of RLS and LMS under different signal lengths (second)

	Number of Signal Lengths (sample)					
Methods	**1000**	**5000**	**10000**	**50000**	**100000**	**500000**
LMS	0.0672	0.308	0.617	3.09	6.26	30.92
RLS	0.122	0.521	1.037	5.211	10.38	53.05

4.9 Conclusion

The medium that has the desired parameters is simulated through the simulation medium developed within the scope of the thesis. The impulse response in the conditions desired can be obtained. Both communication infrastructure as well as the illumination of the medium can be created by using the appropriate LEDs. Having an acute FOV angle generates a better impulse response due to it not receiving the lights that are coming as reflections. However, if the light that is coming perpendicularly is not sufficiently strong, this affects the impulse response negatively. In order for the minimum generation of ISI, no obstruction should be present between the receiver and the transmitter for high-speed communication in the VLC systems.

The basic reason for the ISI is the different arrival times of each signal as the signals coming from different sources follow different paths. Especially since the reflection sourced signals travel a longer path compared to lights that come directly, they are far more delayed and this in turn impairs the impulse response. The signal received from the receiver, and the RCF that filters according to the known symbol ratio increases performance. Equalizer must certainly be used for high-speed communication in VLC systems. The DFE type equalizers constitute a good solution. Although the slower running of the RLS and its application as a circuit is difficult as a learning algorithm, it is able to provide convergence in notably short periods. As convergence in shorter periods means less train sequence, the signal to be sent at regular intervals for channel balancing means that there will be more space left for the actual message.

4.10 Future Work

The VLC systems have started to progressively find larger market share. For example, the size of this market in the USA in 2014 is $200 million dollars, and it is forecasted that the market size will reach $3000 million in 2019. Our country will also get its share's worth from these developments. Within this context, enhancement of the speed of VLC systems and securing their stability is still the most important motivation of researchers. When adaptive equalization is used, the possibility of enhancing its communication capacity has been presented within the scope of this thesis. However, different modulation techniques on the other hand have not been elaborated. In our following studies researching of the most ideal modulation techniques for VLC systems are envisaged. It is possible to enhance the communication speeds by using these modulation techniques again with the use of different equalizers.

REFERENCES

[1] Akanegawa, M., Tanaka, Y., & Nakagawa, M. (2001). Basic study on traffic information system using LED traffic lights. *Intelligent Transportation Systems, IEEE Transactions on*, *2*(4), 197-203.

[2] Ulaştırma Denizcilik ve Haberleşme Bakanlığı, www.udhb.gov.tr/doc/UDHAM_DOC/elektronik_haberlesme.docx [Accessed: 20th September 2015]

[3] Rawat, D., Kestwal, M. C., Kumar, A., & Joshi, S. (2013). Comparison and Simulation of Adaptive Equalizer of LMS, RLS algorithm using MATLAB.

[4] The Industrial Design Engineering, http://www.wikid.eu/index.php/Visible_Light_Communication, [Accessed: 20th September 2015]

[5] Fisne, A., & Toker, C. (2015, May). Analysis of clipping noise in visible light communications. In Signal Processing and Communications Applications Conference (SIU), 2015 23th (pp. 1684-1687). IEEE.

[6] Cisco Visual Networking Index: global mobile data traffic forecast update, 2015-2019, Cisco, 2015.

[7] L.T.E. Advanced: Heterogeneous Networks, Qualcomm Inc., Feb. 2010.

[8] Holzmann, G. J., & Pehrson, B. (1995). The early history of data networks. IEEE Computer Society Press.

[9] Clarke, J. (1966). An introduction to communications with optical carriers. Students' Quarterly Journal, 36(144), 218-222.

[10] T. Komine and M. Nakagawa , " Fundamental Analysis for Visible-Light Communication System Using LED Lights ", IEEE Transactions on Consumer Electronics, Vol. 50, no. 1, pp. 100-107, February 2004.

[11] S. Iwasaki, C. Premachandra, T. Endo, T. Fujii, M. Tanimoto, and Y. Kimura. "Visible light road-to-vehicle communication using high-speed camera", in Proc. IEEE IVS'08, June 2008, Eindhoven, Netherlands, pp. 13-18.

[12] T. Komine and M. Nakagawa, “Integrated System of White LED Visible-Light Communication and Power-Line Communication”, Proceedings of IEEE Transactions on Consumer Electronics, Feb. 2003, Vol. 49, pp. 71-79.

[13] N. Kumar, L. A. Nero and R. L. Aguiar, “Visible Light Communication for Advanced Driver Assistant Systems”, The work is part of FCT project VIDAS – PDTC/EEA-TEL/75217, 2006.

[14] I. C. Rust and H. H. Asada, “A Dual-Use Visible Light Approach to Integrated Communication and Localization of Underwater Robots with Application to NonDestructive Nuclear Reactor Inspection”, in Proc. IEEE ICRA’12, May 2012, Saint Paul, MN, USA. pp. 2445-2450.

[15] T. Komiyama, K. Kobayashi, K. Watanabe, T. Ohkubo and Y. Kurihara, “Study of Visible Light Communication System Using RGB LED Lights”, in Proc. IEEE SICE’11, Sept. 2011, Tokya, Japan. pp. 1926 – 1928.

[16] D. K. Son, E. B. Cho and C. G. Lee, “Demonstration of visible light communication link for audio and video transmission”, in Proc. IEEE PGC’10, Dec. 2010, Singapore. pp. 1-4.

[17] J. Y. Joo, S. K. Lee, C. S. Kang and S. S. Park, “Design of an Ultra Thin Secondary Lens for Visible Light Communication Based on a White LED”, in Proc. IEEE ISOT’09, Sept. 2009, Istanbul, Turkey. pp. 140-145.

[18] Komine, T., Lee, J. H., Haruyama, S., & Nakagawa, M. (2009). Adaptive equalization system for visible light wireless communication utilizing multiple white LED lighting equipment. Wireless Communications, IEEE Transactions on, 8(6), 2892-2900.

[19] Tronghop, D., Hwang, J., Jung, S., Shin, Y., & Yoo, M. (2012, February). Modeling and analysis of the wireless channel formed by LED angle in visible light communication. In Information Networking (ICOIN), 2012 International Conference on (pp. 354-357). IEEE.

[20] Bandara, K., & Chung, Y. H. (2012, October). Reduced training sequence using RLS adaptive algorithm with decision feedback equalizer in indoor visible light wireless communication channel. In ICT Convergence (ICTC), 2012 International Conference on (pp. 149-154). IEEE.

[21] Haigh, P. A., Ghassemlooy, Z., Rajbhandari, S., Papakonstantinou, I., & Popoola, W. (2014). Visible light communications: 170 Mb/s using an artificial neural network equalizer in a low bandwidth white light configuration. Lightwave Technology, Journal of, 32(9), 1807-1813.

[22]Sarbazi, E., Uysal, M., Abdallah, M., & Qaraqe, K. (2014, July). Indoor channel modelling and characterization for visible light communications. In Transparent Optical Networks (ICTON), 2014 16th International Conference on (pp. 1-4). IEEE.

[23] Nguyen, H. Q., Choi, J. H., Kang, M., Ghassemlooy, Z., Kim, D. H., Lim, S. K., & Lee, C. G. (2010, July). A MATLAB-based simulation program for indoor visible light communication system. In Communication Systems Networks and Digital Signal Processing (CSNDSP), 2010 7th International Symposium on (pp. 537-541). IEEE.

[24] Cossu, G., Khalid, A. M., Choudhury, P., Corsini, R., & Ciaramella, E. (2012). 3.4 Gbit/s visible optical wireless transmission based on RGB LED. Optics express, 20(26), B501-B506.

[25] Haigh, P. A., Ghassemlooy, Z., Rajbhandari, S., & Leitgeb, E. (2014, June). A 100 Mb/s visible light communications system using a linear adaptive equalizer. In Networks and Optical Communications-(NOC), 2014 19th European Conference on (pp. 136-139). IEEE.

[26] Shrestha, A. (2009). Visible-Light Communication Demonstrator: System modeling and analogue distribution network design (Doctoral dissertation, MS thesis, Dept. Electrical and Computer Engineering, Jacobs Univ., Bremen, Germany).

[27] Fath, T. C. M. (2014). Evaluation of spectrally efficient indoor optical wireless transmission techniques.

[28] Visser, A. J. W. G., & Rolinski, O. J. (2010). Basic photophysics. American Society for Photobiology.

[29] Y. Ohno (2004), "Color Rendering and Luminous Efficacy of White LED Spectra" , Proceedings of IEEE SPIE - the International Society for Optical Engineering, Vol. 5530, pp. 88-98 (2004).

[30] Wikpedia, www.en.wikipedia.org/wiki/Light-emitting_diode, [Accessed: 20th September 2015]

[31] Cui, K., Chen, G., He, Q., & Xu, Z. (2009, August). Indoor optical wireless communication by ultraviolet and visible light. In SPIE Optical Engineering+ Applications (pp. 74640D-74640D). International Society for Optics and Photonics.

[32] F.J. Lopez_Hernandez, "Low-Cost Diffuse Wireless Optical Communication System based on White LED", in Proc. IEEE ISCE'06, Sept. 2006, St. Petersburg, Russia, pp. 1-4.

[33] J. K. Sheu, S. J. Chang, C. H. Kuo, Y. K. Su, L. W. Wu, Y. C. Lin, W. C. Lai, J. M. Tsai, G. C. Chi, and R. K. Wu. "White-Light Emission From Near UV InGaN–GaN LED Chip Precoated With Blue/Green/Red Phosphors", in Proc. Photonics Technology Letters, IEEE. Jan. 2003, Vol. 15, pp. 18-20.

[34] X. He, G. Cao, and N. Zou, "Simulation of white light based on mixed RGB LEDs", in Proc. IEEE ICCTA (IET), Oct 2011, Beijing, China, pp. 961-964.

[35] Berman, S.,Human Electroretinogram Responses to Video Displays, Fluorescent Lighting and Other High Frequency Sources, Optometry and Vision Science, cilt 68, sf. 645-662, 1991.

[36] Harrington, L.; Bassi, C.; Peck, C., Luminous efficiency and the measurement of luminous efficiency and the measurement of daytime displays, signals, and visors, Aviation, Space, and Environmental Medicine, cilt 76, sayı 5, 2005.

[37] Joseph C. Palais (1988) , Fiber Optic Communications second Edition, Second edition. Prentice Hall.

[38] Komine, T.; Nakagawa, M., Performance evaluation of visible-light wireless communication system using white LED lightings, Computers and Communications, Ninth International Symposium on, cilt 1, sf.258-263, 2004

[39] Lee, K., Park, H., & Barry, J. R. (2011). Indoor channel characteristics for visible light communications. Communications Letters, IEEE, 15(2), 217-219.

[40] Lee, K., & Park, H. (2011, August). Channel model and modulation schemes for visible light communications. In Circuits and Systems (MWSCAS), 2011 IEEE 54th International Midwest Symposium on (pp. 1-4). IEEE.

[41] Moreira, A. J., Valadas, R. T., & de Oliveira Duarte, A. M. (1997). Optical interference produced by artificial light. Wireless Networks, 3(2), 131-140.

[42] Rogers, D. L. (1991). Integrated optical receivers using MSM detectors. Lightwave Technology, Journal of, 9(12), 1635-1638.

[43] Ertürk, S. (2010). Sayısal haberleşme. Birsen Yayınevi.

[44] Haykin, S. (2002) Adaptive Filter Theory, 4th Ed., Prentice-Hall, Upper Saddle River, New Jersey.

[45] Tiryaki S, Hatun, M., and Kocal O.,H."Yeni Bir Adaptif Filtreleme Yöntemi: Hibrid Gs-Nlms Algoritması.", Uludağ Üniversitesi Mühendislik-Mimarlık Fakültesi Dergisi, 13(2), 85-97, 2008

[46] Ablameyko, Sergey.(2003) Limitations and future trends in neural computation. IOS press.

CURRICULUM VITAE

I received my BS degree in Electrical and Electronics Engineering Departmant from Near East University. My research interests include communication theory, signal processing, optical communication.